Design of a Left Ventricular Assist Device:

Heart Turcica Centrifugal

by

Emre Bıyıklı

A Thesis Submitted to the

Graduate School of Engineering

in Partial Fulfillment of the Requirements for

the Degree of

Master of Science

in

Mechanical Engineering

Koc University

July 2009

Koc University

Graduate School of Sciences and Engineering

This is to certify that I have examined this copy of

a master's thesis by Emre Biyikli

and have found that it is complete and satisfactory in all respects,

and that any and all revisions required by the final

examining committee have been made.

Committee Members:

İsmail Lazoğlu, Ph.D. (Advisor)

İskender Yılgör, Ph.D.

Erdem Alaca, Ph.D.

Seda Kızılel, Ph.D.

Halil Kavaklı, Ph.D.

Date: 31.07.2009

Abstract

Left ventricular assist devices (LVADs) are highly needed to use against cardiovascular diseases which are statistically the number one cause of death worldwide. In this respect, development of a Heart Turcica Centrifugal (HTC), which is composed of a continuous centrifugal blood pump (CBP), is very significant for patients with cardiovascular disease. In development of such a device, design phase is highly challenging due to both mechanical and medical constraints such as the need of a small-size, high efficiency and biocompatibility. In order to satisfy the entailed design features, a regular flow within the pump is inevitable. Since the flow behavior is mainly governed by the geometry of the pump, the design tools utilized in determining the values of geometric design parameters were investigated. Design tools included one-dimensional (1-D) design procedure, Computational Fluid Dynamics (CFD) analyses and trial and error method. In the investigation design tools, Computer Aided Design, Engineering and Manufacturing (CAD/CAE/CAM) tools were utilized. 1-D design procedure was found to be unable to provide assistance to design since operating conditions of CBPs fall out of the valid range of the theory. CFD analyses were found to be incapable of assisting the design by means of determining the values of geometric design parameters because the tool could not predict the experimentally measured hydraulic performance of many designs. In contrast, trial and error method initiated with an inspiration from the findings of previous studies was quite successful in designing a CBP. An initial pump, Model 3, was manufactured with values of geometric design parameters adjusted with respect to the previous findings in the literature. Based on the experimental results of Model 3, Model 4 was manufactured with change of control parameter, impeller outer diameter, in accordance with the affinity laws. Model 4 achieved required operating conditions (5 L/min flow rate against a pressure difference of 100 mm-Hg) at a rotational speed of 3000 rpm. Further flow analyses of the pump were conducted with CFD analyses after validating the tool

with successful prediction of experimentally measured hydraulic performance. Analyses of shear stress and velocity vectors pointed no risks of hemolysis or thrombogenicity. The proposed design methodology was, thus, successfully applied and yielded satisfactory results.

Acknowledgements

First of all, I would like to express my respectful gratitude to my advisor, Assoc. Prof. İsmail Lazoğlu, for his great supervision and endless support. This work could not be accomplished without his insight, patience, enthusiasm and extensive knowledge.

I am grateful to kind helps of Prof. Dr. Süha Küçükaksu, Assoc. Prof. Metin Muradoğlu, Asst. Prof. Murat Sözer, Instructor Emel Yılgör, Prof. İskender Yılgör, Asst. Prof. Funda Acar Yağcı, Yasemin Yar and Technician Selim Ölçer.

I would like to thank to my current and former project teammates Çınar Ersanlı, Deniz Erbulut, Fatih Şenbabaoğlu, Gökhan Yıldız and especially Onur Demir in passing his experience on to me.

Thanks go to my friends in MARC research group and around.

Supports of Tübitak and Koç University Engineering Faculty are greatly appreciated.

Last, but not at least, sincere thanks to my family.

Table of Contents

List of Tables

List of Figures

Nomenclature

d_2	impeller outer diameter [m]
g	gravitational acceleration [m/s^2]
H_{des}	desired head [m]
H_{th}	theoretical head [m]
N	rotational speed [rpm]
n_q	specific speed [dimensionless]
Q_{des}	desired flow rate [L/min]
S_{scalar}	scalar shear stress [Pa]
k	turbulence kinetic energy [m^2/s^2]
u	velocity vector [m/s]
x	displacement vector [m]
H	head [m]
β_{2B}	blade outlet angle [degree]
δ	Kronecker's delta [-]
η	molecular stress [Pa]
η_h	hydraulic efficiency [dimensionless]
μ	dynamic viscosity [Pa.s]
μ_t	turbulent viscosity [m^2/s]

ρ	density [kg/m^3]
σ	shear stress [Pa]
τ	Reynolds stress [Pa]
ψ_{opt}	head coefficient at operating point [dimensionless]

subscript *i*	component in the x direction
subscript *j*	component in the y direction
subscript *k*	component in the z direction

Chapter 1 - Introduction

A blood pump is a mechanical device that is utilized in a broad range of medical applications to transport the blood by increasing its pressure. Blood pumps are employed for percutaneous cardiopulmonary support in emergency cases, extracorporeal circulation in surgeries, ventricular assistance in heart recovery or bridge to transplantation and in total artificial heart (TAH) practices [1]. According to Nose, development of blood pumps was progressed in the role of two-day, two-week and two-year pumps where left ventricular assistance falls into the category of two-year long-term circulatory support [2]. Among these applications and phases of development, long-term ventricular assistance was the intended application of the blood pump developed in this project.

In ventricular assistance, blood pumps are equipped in Left Ventricular Assist Devices (LVADs), Right Ventricular Assist Devices (RVAD) and Biventricular Assist Devices (BVAD). In all of these three applications, the heart is not taken out of the body but the devices function in line with the heart. If the blood pump is designed to assist the systemic circulation, which is the loop that provides oxygenated blood to the cells and located between the left ventricular and the aorta, the device is called LVAD. If the blood pump is designed to assist the pulmonary circulation, which is the loop through the lungs where blood is oxygenated and located between the right ventricular and the pulmonary artery, the device is called RVAD. If two blood pumps are employed to assist the both circulatory systems and located both after the left ventricular and right ventricular, the device is called BVAD. Rather than assisting applications, if the heart is taken out of the body and two blood pumps are designed together to imitate the function of the heart, the device is called TAH. The interest in this project was mainly focused on development of an LVAD, which is named as the Heart Turcica Centrifugal (HTC).

Blood pumps are very important for the humanity since the cardiovascular diseases are the number one cause of death and disabilities in the world according to the statistics of World Health Organization [3]. In 1995, 30% of the global deaths are caused by cardiovascular diseases – approximately 15 million people [4]. The situation is a lot worse in Turkey compared to global statistics because the rate of the deaths caused by cardiovascular diseases is 47% as stated by The Ministry of Health of Turkey [5]. LVADs have been used around 5000 and 20 cases in worldwide and Turkey up to date, respectively. In addition, most of the failures in these cases were caused of physiological reasons rather than due to a malfunction of devices. In Turkey, 500.000 people suffer from heart failure every year and 2000-3000 of these people need heart transplantation [6]. However, the need of heart transplantation is not satisfied due to inadequate number of donors. Therefore, the people waiting for heart transplantation require LVADs in order to extend the waiting time before they die. On the other hand, poor people cannot afford the high prices of imported LVADs for the heart recovery or bridge to transplantation applications. That is why the development of Heart Turcica Centrifugal is also aimed to provide cheaper devices for Turkish people since the cost of a device from abroad costs over $ 150.000.

Throughout the development of blood pumps, several types of devices have come forward such as pulsatile blood pumps, continuous centrifugal blood pumps and continuous axial blood pumps [7]. Continuous centrifugal blood pumps (CBP), among these devices, have gained more attention for three main reasons: (i) they are more durable [8], (ii) more efficient [9] compared to continuous axial blood pumps and (iii) they are less prone to failure due to smaller number of moving parts compared to pulsatile devices [7]. Rotary (centrifugal and axial) blood pumps were also categorized in three generations with respect to the advanced features incorporated into the devices [10]. First generation pumps are positive displacement pulsatile devices with valves and a moving chamber. In contrast, second and third generation pumps are continuous-flow rotary pumps of which the only rotating part is the impeller. Second-generation

pumps employ a blood immersed mechanical bearing. The actuation of the impeller of second generation pumps may either be through a shaft or with magnetic coupling. The third-generation pumps employ magnetic levitation in addition to second-generation pumps so that there are no mechanical bearings used in the pump. Among the types and generations of devices, our concern is limited to continuous centrifugal blood pumps of second-generation.

CBPs utilize centrifugal force which is defined as an action that causes an object to move outward from the center of rotation. In CBPs, this feature is adopted to the fluid so that the fluid sucked from the inlet of the pump is moved through the outlet by the rotational movement of the impeller. The impeller of the pump has blades and passages between the blades. The fluid is transported through the passages while an amount of energy is added to the fluid by the blades. The kind of the energy added is kinetic since the velocity of the fluid increases by the rotational movement of the blades. The fluid is then slowed down between its discharge from the impeller and outlet of the pump. Therefore, the kinetic energy of the fluid is converted into the pressure with respect to Bernoulli's principle which states that an increase in the speed of the fluid occurs simultaneously with a decrease in pressure or vice versa. The amount of energy added by the impeller is directly proportional to the rotational speed of the impeller. This way, operating conditions of the blood pumps are easily adjusted for different applications by the control of the rotational speed of the impeller. LVADs too utilize this specialty via a speed controller located outside of the body for different operating conditions required. In normal circumstances, the operating conditions of continuous LVADs are set to provide the required hydraulic performance for a healthy systemic circulation, which is 5 L/min flow rate against a pressure of 100 mm-Hg. That is why one of the important features an LVAD have to possess is to provide the required hydraulic performance.

Development of a CBP entails many features to be incorporated into the system. These features were well established in seven items by Nose et al.; (i) small size, (ii) atraumatic features, (iii) anti-thrombogenic features, (iv) anti-infectious features, (v) durable and simple design, (vi) low energy requirement and (vii) easy controllability [11]. Incorporation of these features are, however, challenging due to both mechanical and medical constraints. Mechanical constraints involve obtaining required hydraulic performance with small sizes. In addition, durability for a long-term support of at least two years non-stop performance is also a critical mechanical constraint for CBPs. Medical constraints are the risk of hemolysis which is the destruction of blood cells due to high shear stress in the flow; the risk of thrombogenicity which is the coagulation of blood (clot formation) due to flow stagnation; and low energy requirement due to undesired excessive heat dissipation from the implanted device to the body.

The challenges in the development of CBP are initially confronted at the design level. These challenges are most related to the behavior of the fluid flow within the pump such that the risks of hemolysis and thrombogenicity increase where the flow is disordered. The distortion of the flow also hardens to overcome mechanical challenges caused by reduced efficiency. In order to overcome these problems, it is inevitable that the flow within the pump has to be regular. This flow behavior is mainly governed by the pump geometry. The extrusion of the pump geometry is the main consideration of the design and includes the determination of the values of geometric design parameters. However, this is a very difficult task due to the vast number of geometric design parameters since it is practically impossible to manufacture all possible pump combinations with various values of geometric design parameters. At this point, some kind of assistance in dealing with geometric design parameters should be introduced such that the designer should have either guidance or enough experience in design of CBPs.

This research was mainly composed of evaluating many of the design tools so far have been used in design of CBPs. In doing so, design tools of One-Dimensional (1-D) design procedure, Computational Fluid Dynamics (CFD) analyses and trial and error method were reviewed and a design methodology to be employed in extrusion of the pump geometry at the design level of the development of CBPs was addressed. The applicability of 1-D design procedure to provide an initial idea for determination of values of geometric design parameters was analyzed by comparing the operating conditions of blood pumps to the valid ranges of 1-D design theory. Use of CFD analyses as a design assistance tool in determination of the values of geometric design parameters was investigated via comparison of hydraulic performances tested experimentally and predicted by CFD analyses. The method of trial and error initiated with an inspiration from the previous findings in the literature was studied by initializing a design with particular previous studies followed by manufacturing and testing of several pumps experimentally.

In the investigation of design, computer aided design (CAD), engineering (CAE) and manufacturing (CAM) tools were utilized. The pumps were fabricated from Poly Methyl Methacrylate (PMMA) in high precision by using a high speed computer numerical controlled (CNC) machine and then hydraulic performances were tested in the experimental setup. Experimental test setup consisted of a closed loop circuit with reservoir, pressure sensors and motor. A computer and DAQ card was integrated into the system to read and monitor the data from the pressure sensors. Experimental tests were conducted with both water and blood analog as the medium.

The design tools 1-D design procedure and CFD analyses were found to be inapplicable and immature to guide the designer in determining the values of geometric design parameters, respectively. In comparison, trial and error method subsequent to an initial set of most of the values of geometric design parameters with respect to the outcomes of the previous studies was proven to handle the design process well. After

an initial idea about the values of geometric design parameters was gathered from the previous studies, two pumps were designed, manufactured and tested experimentally. With the second pump, required hydraulic performance was achieved with preferable pump sizes. Moreover, CFD analyses were employed in investigation of the pump's inner flow and provided useful information about the flow behavior of the second pump after validation of the analyses with experimental hydraulic performance results. As a result, hemolysis and thrombogenicity analyses of the second pump were satisfactory. The study pointed out to the conclusion that design of CBPs should be initiated with a well understanding and following of previous studies, preceded with few trials of manufacturing and utilized from CFD analyses (if they were validated) to investigate the pump's inner flow.

The introduced design methodology renders that CBPs with small sizes and satisfactory hydraulic performances with no serious harm to blood can easily be designed. This way the study is most beneficial in enlightening a beginner designer with no experience. On the other hand, all the work accomplished provided an important amount of experience and know-how so that development study of LVAD will be continued more effectively. This way, blood pumps in smaller sizes to be implanted in small-sized and pediatric patients would be developed. Besides, blood pumps with higher efficiency would be designed so that expense of energy would be reduced. Hence, the undesired heat dissipated to the body would be reduced. In addition, the batteries would have longer working time which provides ease of use.

Chapter 2 covered the previous studies on the field with a comprehensive literature review. Presentation started with a review of historical background, followed by a look into design and tools employed in design. In addition, the methods and tools utilized in CAE studies were analyzed. In the same way, experimentation techniques applied in previous studies were brought into the attention.

Chapter 3 introduced the tools and methods readily or planned to be employed in development of HTC. In this respect, CAD/CAE/CAM tools were described in details. Moreover, details of manufacturing and experimentation procedure in addition with the utilized materials were introduced. In the last section of the chapter, the investigated design tools: 1-D design procedure, CFD analyses and trial and error method were explained.

In chapters 4 and 5, the results emerged from investigation of design tools 1-D design procedure, CFD analyses and trial and error method were manifested and discussed, respectively. The results covered testing of the ability of design tools in determining values of the geometric design parameters. On the other hand, the indications of the results as well as the advantageous and disadvantageous of the design tools were cited in discussion.

Chapter 6 presented the end of the work with concluding remarks followed by future work of the project.

Chapter 2: Literature Review

In this chapter, a comprehensive literature survey about blood pumps is presented. In the first section, the history of blood pumps is provided. Later, the design of Centrifugal Blood Pumps (CBPs) is reviewed through articles which study different values of geometric design parameters. In the design tools section, the tools utilized in the literature for the design of CBPs were discussed. Computer Aided Engineering (CAE) section covers the details of Computational Fluid Dynamics (CFD) analyses applied by other researchers. Lastly, information regarding to the experimentation conducted in other studies and utilized in the experimentation level of the current project was introduced.

2.1. Historical Background

This section provides information about historical background of Mechanical Circulatory Support (MCS) and so the devices. Looking at back to the history, milestones of the struggle of mankind against heart diseases was listed as in Table 1. The events listed on the Table 1 were first appeared in the cited year. MCS was begun in 1953 with the work of Gibbon who first applied cardiopulmonary bypass [12]. In 1966, DeBakey had reported use of a ventricular assist device for postcardiotomy support for ten days [13]. Meanwhile, first human-to-human heart transplantation was accomplished by Christian Bernard [13]. After a short time (1969), a TAH implantation was performed by Dr. Denton Cooley in Texas [14]. Ten years later (1979), biventricular bypass was conducted by employment of two rotary blood pumps [14]. Despite all the research and development of MCS devices listed above; on the other hand, these devices have been used in a lot of medical cases up to date [14]. In these

applications, the ratios of implementation of blood pumps in MCS devices are as illustrated in Figure 1 [14].

Table 1: Milestones in struggle against heart diseases

Year	Event	Who
1895	Cardiac surgery	Axel Cappelon
1953	Mechanical circulatory support	Gibbon
1966	Successful use of LVAD	DeBakey in Baylor College of Medicine, Texas, USA
1967	Human-to-human heart transplantation	Christiaan Barnard
1969	TAH implantation	Dentan Cooley
1979	BVAD implantation	Murakami et al.

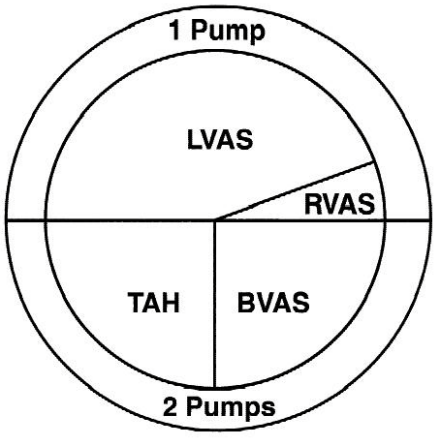

Figure 1: Applications of blood pumps in MCS devices

Types of the blood pumps employed in MCS devices were widely pulsatile until 1990s [14], even though the idea of continuous blood pumps was first described by Saxton and Andrews in 1960 [7]. However, the attention to these devices has increased in the last 20 years and the superiority of continuous blood pumps were well described in numerous recent articles. As stated earlier, pulsatile pumps were categorized as first-generation pumps; and continuous-flow rotary blood pumps were as second and third generation pumps according to the type of levitation they utilize. The generations and types of the major commercially available devices are as in the Table 2 [7].

Table 2: Types and generations of major pumps

First-generation	Second-generation	Third-generation
CardioWest TAH	MicroMed DeBakey VAD	Terumo VAD
Thoratec BVAD	Jarvik 2000 VAD	MedQuest HeartQuest VAD
TCI HeartMate I VAD	Nimbus-TCI HeartMate II VAD	Uni. of Pittsburgh Streamliner VAD
Novacor VAD		

In addition to three generations of blood pumps stated above, there is a fourth-generation patented by Olsen. The fourth-generation blood pumps intend to utilize the magnetic property of ions existing in the blood. Hence, the idea aims to move the blood by enforcing magnetic force on the ions so that no use of any impeller will be necessary. However, the inadequate number of ionic molecules within the pump remains as the problematic issue in the subject [7]. Despite the fact that the generations of blood pumps were constructed with respect to the advanced features incorporated

into the devices, the ongoing research of blood pumps have not totally been focused on third-generation blood pumps. The underlying reason for the current research both on second-generation and third-generation blood pumps is that the feasibility of developing a third-generation blood pump is still controversial since the required effort for developing a third-generation blood pump is much more compared to developing of a second-generation blood-pump [10].

The development times of types of two-day, two-week and two-year blood pumps in Baylor College of medicine were presented by Nosé et. al [14]. According to this report, development of two-day and two-week pumps lasted 4 and 6 years, respectively. In addition, development of long-term pulsatile, long-term axial and long-term centrifugal blood pumps required an expense of 15, 10 and 10 years in overall, respectively. The study also anticipated that conversion of a laboratory blood pump to a clinically applicable one, as part of the overall development period, takes 1 year for a two-day blood pump, 2 years for a two-week blood pump and 5 years for a long-term support blood pump.

New technologies besides the magnetic levitation such as the trans-percutaneous energy transmission, which enables transfer of energy over the skin so that eliminates the need for percutaneous cables, are incorporated in recently developed blood pumps [15]. Utilization of new technologies in blood pumps demonstrates the amount of work conducted on development and indicates the necessity for development of blood pumps. Today, there are more than 10 pumps being developed and most of which were approved and commercially available. The development of Heart Turcica Centrifugal (HTC) is in the stage of in-vitro tests after two and a half years of research. The current state and next milestones of the project are discussed widely in conclusions and future work.

2.2. Design

Most of the studies about design of CBPs in the literature were focused on identifying the effects of geometric design parameters. Many other articles were also concentrated on different types of impellers (open or shrouded) and pumps (centrifugal or axial). However, the work presented herein presents studies which include information about CBPs since CBPs are the main consideration of this thesis project as mentioned earlier. In this respect, summaries of articles which have studied effects of different values of design parameters are listed in Table 3.

Table 3: Design studies

Geometric design parameters	Comparison	Tool	Result	Ref
• Blade exit height (1, 2, 3 mm) • Blade shape (varying curvatures) • Open vs. shrouded impeller	• Hydraulic performance	CFD	• 3 mm • Compromise between straight and slightly curved • Open	[16]
• Blade height (4, 8 mm) • Blade shape (straight, curved)	• Hydraulic performance • Hemolytic performance	Experimental	• No difference • Straight	[17]
• Radial gap (0.5, 3 mm) • Axial gap (0.5, 1, 1.5 mm) • Blade shape (straight,	Hemolytic performance	CFD (validated with flow visualization)	• 3 mm • 1 or 1.5 mm • Straight	[18]

backward)				
• Radial gap (0.5, 1.5, 3 mm) • Axial gap (0.5, 1, 1.5 mm) • Blade shape (straight, backward, forward, winding)	Hemolytic performance	Experimental	• 3 mm over 1.5 mm; 1.5 mm over 0.5 mm • 1 or 1.5 mm • Straight	[19]
• Radial gap (0.5, 1, 2, 3 mm) • Outlet port position (standard, outward) • Blade shape (straight, backward, forward, winding)	Hemolytic performance	• In-vitro • Flow visualization • CFD	• 1 or 2 or 3 mm • No difference • No difference	[20]
• Pump type (centrifugal, axial)	Hemolytic performance	Experimental	Both are OK	[2]
• Radial gap (0.5, 3 mm) • Outlet port position (standard, tangential) • Washout holes (with, without)	• Hemolytic performance • Hemolytic performance • Flow stagnation	CFD	• 3 mm • Tangential • With washout holes	[21]
• Blade shape (straight, forward, backward) • Blade number (less, more)	• Hydraulic performance	Experimental	• Straight or forwards • More	[4]
• Blade shape (straight, backward)	• Hydraulic performance • Hemolytic performance	CFD (validated with flow visualization)	• Straight • No difference • No difference	[22]

	• Flow stagnation			
• Volute design technique (constant angular momentum, constant mean velocity)	• Hydraulic performance • Hemolytic performance	CFD (validated with experimental hydraulic performance)	• Constant angular momentum	[23]
• Front and back clearances between impeller and housing (0.01, 0.02, 0.03 inch)	• Hydraulic performance • Hemolytic performance	CFD	• 0.01inch • No difference	• [24] • [25] • [9]
• Blade angles at inlet and outlet (I: 65°-81°, II: 25°-61.5°)	• Hydraulic performance • Streamlines • Hemolytic performance	• Experimental • Flow visualization • Experimental	• I by compromise	[26]
• Radial gap (0.5, 3 mm) • Axial gap (0.5, 1.5 mm) • Outlet port position (27.5, 30.5 mm)	• Hydraulic performance • Velocity vectors • Hemolytic performance	• Experimental • Flow visualization • Experimental	• Small radial gap is the problem • The others have no major effect	[27]
• Washout holes (with, without)	• Flow stagnation	CFD	• With washout holes	[28]
• Radial gap (6, 11 mm) • Axial gap (0.5, 1, 1.5, 2, 2.5, 3 mm) • Blade shape (straight radial, straight inclined, curved)	• Hydraulic performance • Hemolytic performance	• Experimental • Experimental	• 6 mm • 1.5 mm • Straight radial	[29]

The first column of the Table 3 contains the parameters of the geometric design, or types of parts of pump, or techniques. The parameters include blade shape, blade height, blade angles, blade number, impeller type, pump type, radial and axial gaps, front and back clearances between the impeller and the housing, outlet port position, volute design technique and washout holes. The criteria by which the effects of different parameters were evaluated are placed in the second column such as hydraulic performance, hemolytic performance, flow stagnation, streamlines, or velocity vectors. The third column contains information about the tool employed in comparing the effects of different parameters by means of the criteria presented in the second column. The tools are experimental, computational (CFD) and/or visual. The results of many studies containing CFD tool are controversial since they did not provide any validation before use of this tool. Hence, the studies containing validation of this computational tool are noted exclusively. The fourth column presents the successful results such that the value of the parameter that is superior to the compared ones is written in this column. The studies are referenced in the last column. The tools presented in column three will be discussed in the next section of this chapter widely.

2.3. Design Tools

Numerous studies have been reported related to the design process of CBPs. Most of these studies concentrated on the effects of geometric design parameters on performance of the blood pump as presented in the previous section of this chapter. One important notification about these studies is that they had presented the effects of different values of geometric design parameters as the results. However, there were no evidences of any reasoning in the first place in determining the values of geometric design parameters to be studied later. At this point, it is assumed that the values of

geometric design parameters to be studied were selected appropriately based on the experience of the researcher. The design tools were utilized in evaluating the different designs with different values of geometric design parameters. Many of these tools are one-dimensional (1-D) design procedure, CFD analyses and experimentation.

1-D design is a simple design tool which deals with mean velocities of the real, three-dimensional, viscous flow in the pump. The procedure includes several formulas and charts with empirical coefficients gathered from vast number of experimental data [30,31,32]. Since the tool is based on a simplified theory, it is utilized in initiating a design to give a general idea about the values of the geometric design parameters. A few of the studies in the literature introduced reasoning in determining the initial values of geometric design parameters with 1-D design procedure but the studies were either incomplete [1,16] or limited to the parts of the pump [23].

Most of the researchers employed CFD analyses in later examination of pump's inner flow. Many of these researchers have utilized from CFD analyses after validating the tool by agreement of hydraulic performance with experimental tests [23,33,34], or qualitative analyses of velocity vectors with flow visualization measurements [18,20,22] or both [35]. In many studies, researchers had not shown any validation of CFD analyses so that the reliabilities of the results presented in these studies are obscure [16,19,21,24,28,36]. Details regarding to the conduction of CFD analyses reported in the literature is reviewed later in this chapter, in the next section.

Majority of the studies about design of blood pumps in the literature conducted experimental tests as documented in the previous section of this chapter. Experimental tests do contain the ultimate results and represent the most reliable data. However, experimentation as a design tool has the disadvantage of dealing with limited number of designs since manufacturing and testing of a pump requires considerable amount of time and effort. To sum up, there is not yet any thorough design tool to employ in design of blood pumps in one shot and come up with the expected design in a short

time. This fact was also evidenced by other designers as mentioned in the first section of this chapter.

2.4. Computer Aided Engineering

In the development of HTC, computer aided engineering was utilized by means of CFD analyses. CFD analyses were conducted through simulation tools provided by commercial software packages. These simulation tools ask for the characteristic of the flow phenomena and the fluid geometry. For this, the user specifies the details of the simulation and mesh of the geometry. In this respect, although the software packages offer quite good references, the studies of the colleagues on the same subject provide useful information. However, results of the CFD analyses were rarely validated with the experimental data in the literature, which results in lack of reliability in the presented data. That's why this section covers a few studies in the literature that are validated with the experimental results only. The work presented in this section concentrates on the details of the way of applying CFD tool to simulate the physical phenomena in CBPs.

Oh et. al. [33] validated the correctitude of CFD analyses through successful prediction of the experimental hydraulic performance of the developed pump. ANSYS, as the well-established CFD code, was employed. The pump was defined in three separate geometries of inlet duct, impeller and volute casing which were meshed by 584K tetrahedrons, 885K prisms and 12K pyramids in total. Turbulence model of k-ω based shear stress transport (SST) was chosen in order to obtain highly accurate predictions of the onset and amount of the flow separation under adverse pressure gradient. Total pressure and mass flow rate were defined at the boundary conditions of inlet and outlet, respectively.

Burgreen et. al. [37] also accomplished verification of the correctitude of CFD analyses by successful results of CFD analyses in predicting the experimentally measured hydraulic performance of the pump studied in the report. Fluent, a commercial CFD code, was employed. All the regions that fluid flows through within the pump, including the gaps, were incorporated in the geometry. The geometry was meshed with 325K nodes and 1.4M cells in total. The interfaces between the rotating and stationary regions were modeled with the sliding mesh principle. Time step of the simulations were adjusted as division of one full rotational period into 200 increments.

Chua et. al. [35] validated the correctitude of CFD tool by good agreement of CFD analyses with the experimental hydraulic performance of the pump presented in the study. The commercial CFD code utilized in the study was Fluent. 510K unstructured computational grids were generated for the simulation and k-ω turbulence model was applied. The inlet and outlet of the impeller, which are the interfaces between rotating and stationary regions, were modeled with sliding mesh option to solve the interactions. Time step was adjusted to one-320^{th} of the rotational time. The length of the inlet pipe was prolonged five times the pipe diameter in order to achieve a steady inlet flow.

Zhang et. al. [34] too utilized successful hydraulic performance prediction of the CFD analyses to verify the correctitude of the tool. Fluent was again the commercial CFD package used in the study. All the wet geometry within the pump was modeled, including the gaps. The whole geometry was meshed with 3-D tet/hybrid elements adding up to a number of 1.28 M cells in total. Velocity and pressure of the fluid were defined at the inlet and outlet boundaries of the pump, respectively. Steady laminar flow was assumed and multiple reference frame model was employed to count for the rotational motion.

Many of the arguments regarding to the details of the CFD simulations presented above may be ambiguous in this section alone; but part of these terms, the ones they

were employed in CFD analyses of this project, are explained CAE section of material and methods chapter in detail.

2.5. Experimentation

The experimentation of a designed blood pump in the development of HTC consisted of manufacturing the pump and hydraulic performance testing of the pump in the experimental setup. The experimental setup consists of hardware such as motor, pipes, pressure sensors, fluid etc. The properties of the equipment, the placement of the equipment, or sometimes the equipment itself used in testing the hydraulic performance of a blood pump was partly adjusted with respect to the information gathered from other studies in the field in the literature. This way, the experimental conditions were kept similar so that the results obtained in the tests were comfortably compared to the other findings presented in the literature.

The resistance of the experimental setup to the fluid greatly affects the performance of the pump, especially by means of the maximum possible flow rate. The resistance is mostly governed by the diameter of the tubing employed, the valves and other parts that the fluid passes in or over while flowing within the closed-loop circuit. The resistance of the system may vary in a broad range with different the amount of resistance introduced by the parts listed above. In this respect, it is crucial to set the values of variables similar to those in the literature so that the hydraulic performances of the tested pumps may be compared to the ones presented in the literature.

Most of the experimental setup in the literature consists of tubing of in diameter larger than 3/8” (9.525 mm) inner diameter [19,26,38,39,40,41]. The inner tube diameter was set to 1/2” (12.27 mm) in our experimental setup as was done by Takiura et al. [19] since this study is a good similar study to follow due to its qualification. Two

valves were integrated into the circuit; one at the discharge from the reservoir and the other at the discharge to the reservoir. The latter was utilized to change the resistance of the system so that the hydraulic performance of the pump could be measured at different operating conditions. The number and placement of the valves were adjusted (i) to keep the resistance of the circuit minimum when the valves are at fully open state and (ii) with respect to the instances found in the literature [4,27].

The blood analogous used in the experimental setup as the medium was glycerine/mixture composition as used by many [22,42,43]. The mixture was composed of three parts of water and two parts glycerine as suggested by Yu et. al. [42]. This way, the fluidic properties of blood (density of 1045 kg/m^3 and viscosity of 0.00345 Pa.s) was obtained as defined by Oh et. al. [33].

A new experimental setup is being constructed for in-vitro testing with blood in order to identify the hemolysis tests of developed pumps. In constructing the setup, standards offered by the American Society for Testing and Materials (ASTM) were accounted. Blood that will be used as the medium in the experimental setup is suggested to be fresh, that is use of blood within 48 hours and contain anticoagulants such as citrate phosphate dextrose adenine or heparin sulfate [44]. Test loop is suggested to be consisted of 2 m long, 3/8" (9.525 mm) inner diameter polyvinylchloride tubing and reservoir and 450 ± 45 milliliters blood [45]. The operating conditions are advised as 5 ± L/min flow rate against a pressure head of 100 ± 3 mm-Hg at the circulating blood temperature of 37 ± 1 °C for left ventricular assisting application [45]. In the evaluation part, it is recommended sampling 1 to 2 mL of blood and measurement of hemoglobin, plasma hemoglobin and hematocrit concentrations [45]. After all measurements, Normalized Index of Hemolysis (N.I.H.) is calculated with the proposed equation [45]. In order to conduct the hemolysis tests, more detailed information is required which can be found at the standards [44,45].

The information provided in this chapter was utilized in the materials and methods applied for design, CAE and experimentation of this project. Specifically, the reasons of choosing or adjusting the values of many of the appropriate materials and methods were based on the sources mentioned above. The exercise of the information provided above can be viewed in the materials and methods chapter more precisely.

Chapter 3: Materials and Methods

Materials and methods chapter includes information about the tools and materials utilized in developing the Heart Turcica Centrifugal (HTC) pumps. In this respect, a general characteristic of the HTC pumps and Computer Aided Design (CAD) employed to generate the designs were introduced. Details of performed Computational Fluid Dynamics (CFD) analyses were described. The procedure followed in manufacturing and experimentation was introduced and the tools and materials applied within the procedure such as Computer Aided Manufacturing (CAM) were reported in detail. Finally, design tools which were investigated to determine the values of geometric design parameters and considered as the main part of this research were introduced.

3.1. Computer Aided Design (CAD)

Centrifugal pumps consist of an impeller, a volute and inlet and outlet sections (Figure 2). Impeller is the only moving part (rotational movement) where the others are stationary. When the pump starts to work (when the impeller starts to rotate), it simultaneously starts to suck the fluid from the inlet section through the eye of the impeller. Since the impeller is rotating, the fluid is transported away from the eye of the impeller by centrifugal forces. Meanwhile, an amount of energy is imparted to the fluid so that the velocity of the fluid increases. The fluid is first released from the impeller to the volute of the pump. Volute is the part by which the fluid is channelized to the outlet of the pump for discharge. In volute, the fluid gains pressure while losing velocity according to the Bernoulli’s principle. Last, the fluid is discharged out of the pump from the outlet section.

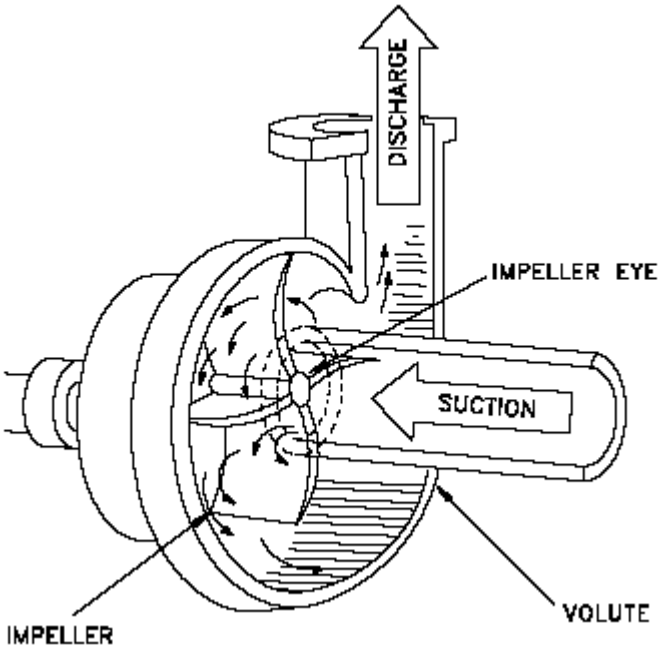

Figure 2: Parts of a centrifugal pump [46]

The impeller and the volute are the fundamental parts of a pump which requires the most work in design. The geometries of an impeller and a volute are depicted in

Figure 3. The type of the impellers considered in design of HTC was open type and had three parts: hub, blades and eye. Hub, as the name implies, acts like a hub so that all other parts are attached to it.

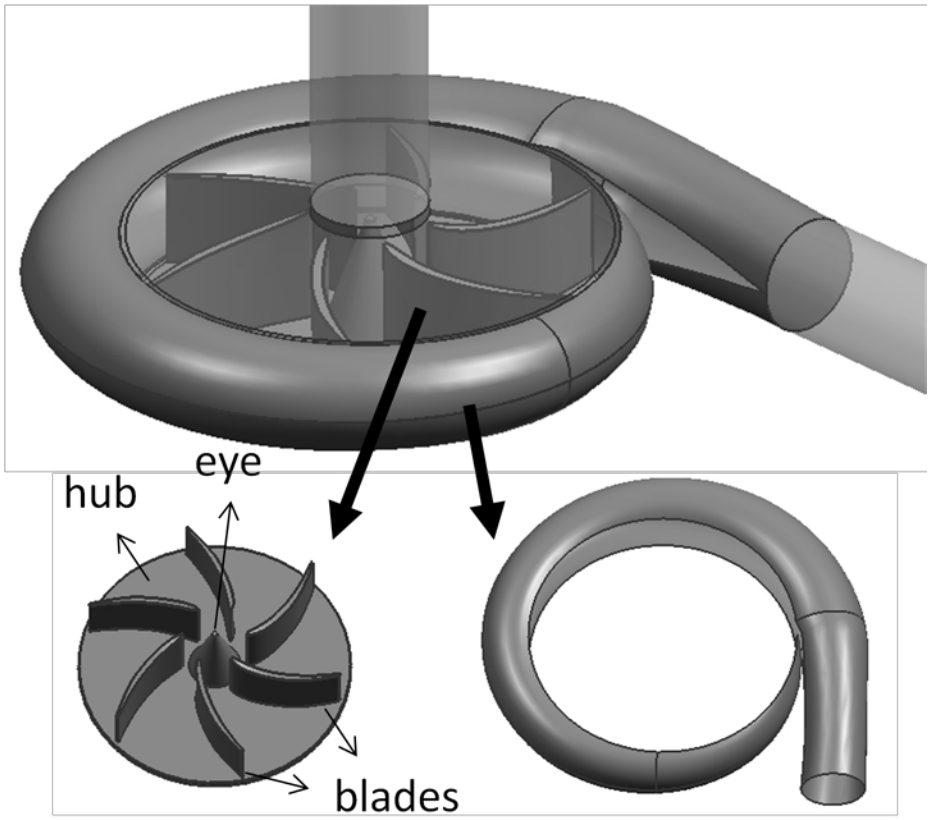

Figure 3: Impeller and volute of a pump

The impellers designed in development of HTC, had axially vertical blades due to sake of easy manufacturing (Figure 4). Right side of the Figure 4 demonstrates the back side of the impeller where the magnets and bearing are embedded. There were 16 magnets inserted into the impeller around a circle of diameter of 35 mm. The magnets, which were 4 mm in both height and diameter, were located in the order of two pole pairs such as north-north-south-south-north-north etc. The bearing that was assembled in the middle of the impeller had a height of 4 mm and inner and outer diameters of 3 and 8 mm, respectively.

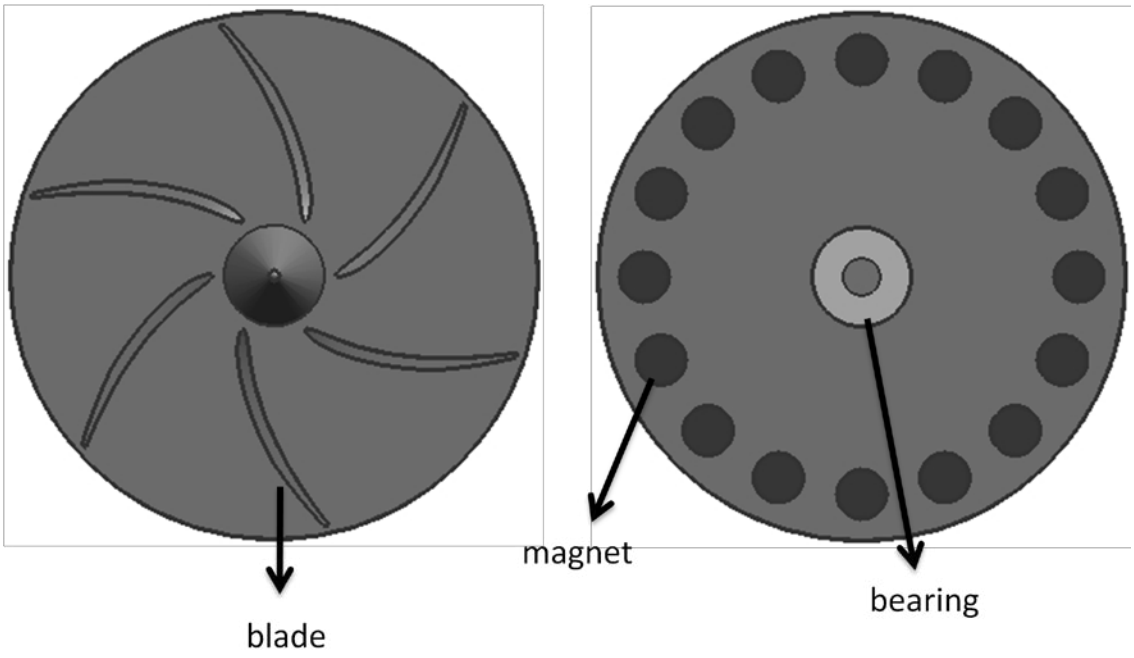

Figure 4: Front and back views of HTC impellers

In many designs, washout holes were located into the impeller in order to impede the flow stagnation between the back-side of the impeller and the housing around the bearing (Figure 5). The locations of the holes were kept close to the bearing so that the fluid inclined to stagnate in the critical region was channelized back to flow forward to the front region of the impeller.

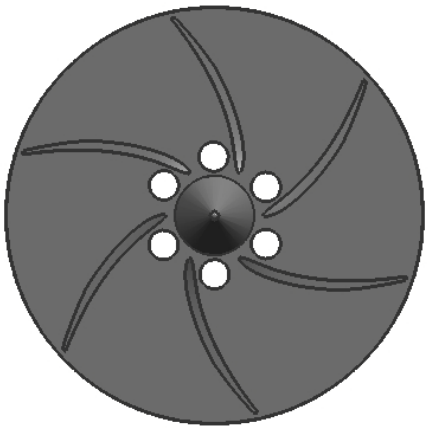

Figure 5: Washout holes

Computer aided design of pumps were realized in Unigraphics which is a very advanced design software. Although the extrusion of the pump geometries were handled easily with this software, curved blade designs as in Figure 4 were conducted with the aid of MATLAB in many cases. In doing so, the points those form the curved blades were first calculated in MATLAB and then transported into the Unigraphics. Later, Unigraphics fits a curve to the desired degree on the points imported.

Extrusion of the volute is different than the impeller because impeller is a solid part while volute is a void in which fluid flows through. Hence, volute is formed via the voids at the caps of the pump as in

Figure 6. The pumps designed in this project were solidified in three parts as impeller, upper cap and lower cap. Volute was formed with voids halves of which were at upper and lower caps. When the caps were assembled through the surfaces which include the voids for volute, the volute was obtained. The outlet of the pump was formed in the same way as volute with half voids at the caps. The inlet was located at the upper cap by an axial thorough hole. Last, the lower cap included a shaft on which

the impeller was mounted. Upper and lower caps form the casing of the pump mutually.

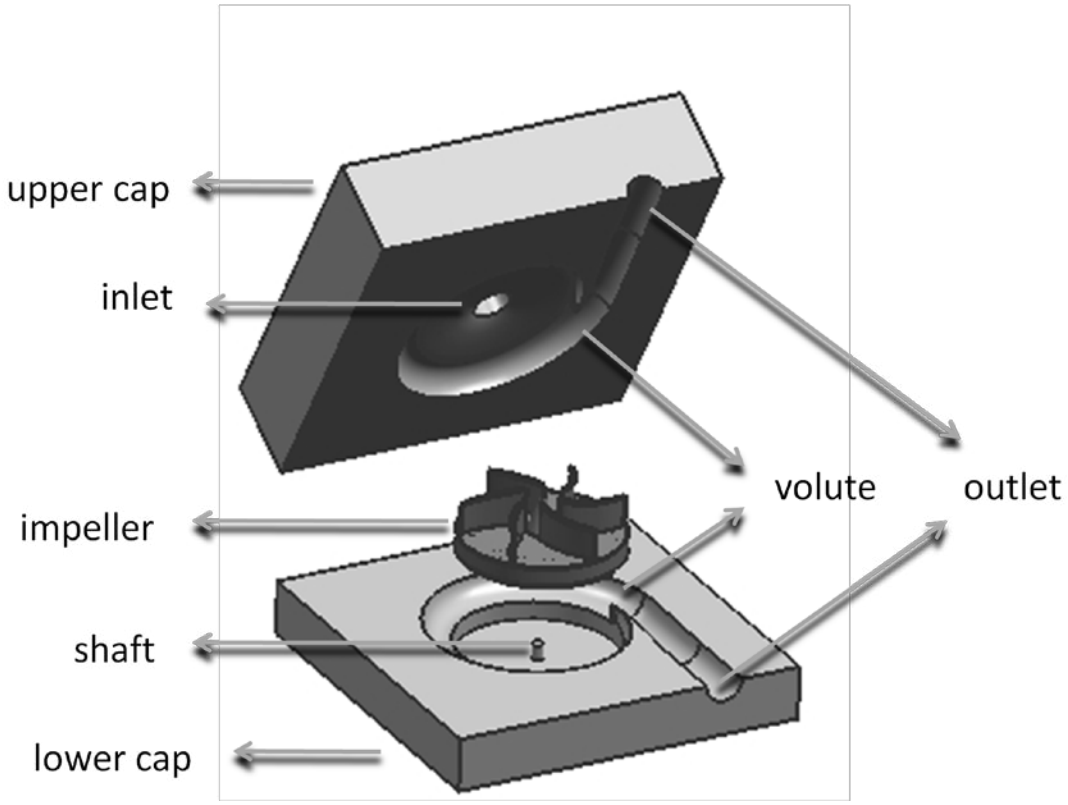

Figure 6: Impeller, lower cap and upper cap of the pump

The gaps in the pump are three types: axial gap, radial gap and back clearance (Figure 7). The axial and radial gaps are especially important in hemolytic performance of the pump while the back clearance is crucial in flow stagnation.

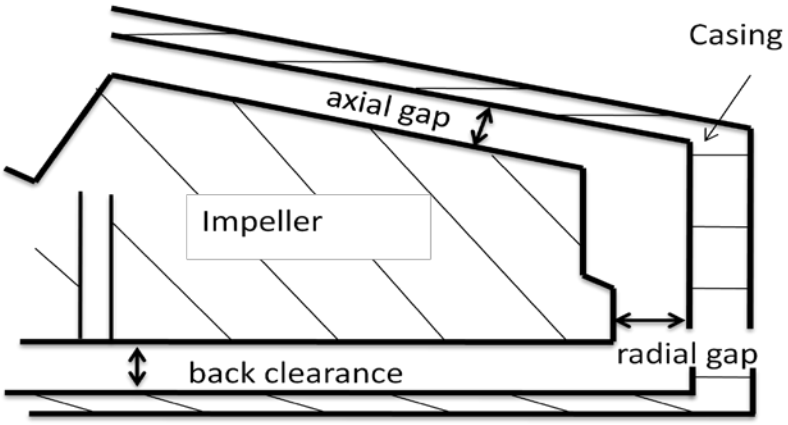

Figure 7: Gaps in the pump

The final design property of HTC pumps was the magnetic coupling by which the impeller is actuated. In magnetic coupling, 16 magnets were places in a circular disk in the same orientation with the magnets in the impeller (Figure 8). This circular disk was mounted around the shaft of the motor so that when the motor starts to rotate, the circular disk rotates too. The magnets within the circular disk couple with the ones in the impeller so that actuates the rotational movement of the impeller.

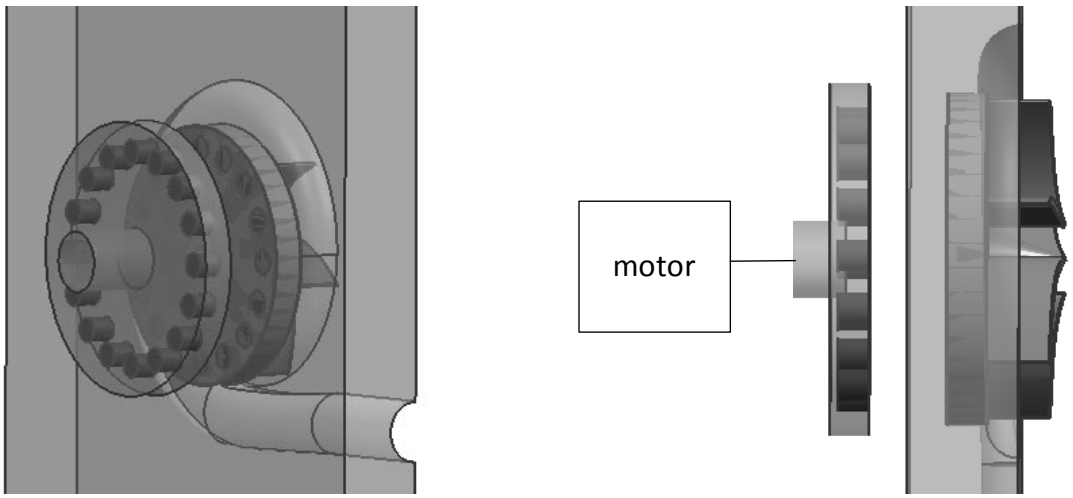

Figure 8: Magnetic coupling

3.2. Computer Aided Engineering (CAE)

In development of HTC, Computer Aided Engineering (CAE) was utilized by means of Computational Fluid Dynamics (CFD) analyses. CFD analyses involved simulation of the actual flow in part of the experimental setup. The part included the fluid between the pressure sensors those were located before and after the inlet and outlet of the pump, respectively. Since the analyses did only concern with the fluid part, the fluid geometries were introduced to the analyses. For this, CAD drawings that only consisted of fluid were exported from Unigraphics in Parasolid format (.x_t) in three parts: inlet, impeller and outlet (this one also included the volute). The fluid geometries in Parasolid format were transported to ANSYS Workbench for meshing, simulations and post-processing.

The fluid geometries in Parasolid format were initially imported into the CFX-Mesh module of ANSYS Workbench. Initially, CAD checking of the geometries was conducted. If any problem encountered in here, the problematic surface or edge was redefined as “virtual face” or “virtual edge”, in order. If the problem was still persisted, redrawing of the geometry in CAD was required. The geometries that were free of error were initially surface-meshed with the following parameters:

Table 4: Surface mesh parameters

Default face spacing	
Option	Angular resolution
Angular resolution [degrees]	30
Minimum edge length [mm]	0.0001
Maximum edge length [mm]	0.00065

The angular resolution allowed edge length to vary depending on the curvature. Hence, the control to resolve the curvature was adjusted by the angular resolution parameter. Angular resolution parameter represented the maximum angle allowed subtended by the arc between two adjacent surface mesh nodes. Minimum and maximum edge lengths controlled the minimum and maximum edge lengths used by the mesher, respectively [47].

Inflation was employed near the walls in order to resolve the boundary layer effect more accurately. In CFX-Mesh, inflation was conducted by using prisms near the inflated boundaries instead of tetrahedrons. Inflated boundaries were introduced as walls near which the boundary layer effect considered important such as volute walls, impeller walls and walls of inlet and outlet close to the pump. In inflation, maximum thickness, that was the only control parameter and defined the thickness at which inflation was active, was set to a value between 0.2 and 1 mm [47].

Figure 9: Surface-meshed impeller geometry in CFX-Mesh

The volume mesh was generated after the surface meshing of the geometry was completed (Figure 9). In volume meshing, a parameter called “body spacing” was introduced so that user was allowed to adjust the maximum spacing. Maximum body spacing represented the maximum value of the body spacing allowed and adjusted to a value near 0.5 mm [47].

In many cases, body spacing and face spacing were slightly modified so that the total number of elements was kept around 1.5 M. The maximum number of elements was kept under the RAM capacity of the computer because otherwise the hardware was being insufficient to process the simulation. Indeed, the number of elements employed was kept higher than the average levels. This way the accuracy of the solution was guaranteed not to be determined by the quality of the meshing by means of element number. After completion of the meshing of geometries, the parts were transported to Advanced CFD module of ANSYS Workbench in *.gtm* file format.

Advanced CFD module of ANSYS Workbench consisted of three parts:

- CFX-Pre: Details of simulation were introduced.
- CFX-Solver: The solution was executed.
- CFX-Post: Results were viewed.

In CFX-Pre, initially, geometries in *.gtm* format were imported and each of them was defined as a region. As a part of determining the properties of regions, the medium (fluid material), reference pressure, buoyancy option, domain motion and turbulence model were set. The medium was either set to water or glycerine/water mixture. While water was an inherent fluid material, glycerine/water mixture was introduced to the Advanced CFD by a new material of which viscosity and density were set to 0.00345 Pa.s and 1045 kg/m^3, respectively. Reference pressure was set to 0 Pa and buoyancy was ignored. Domain motion was set to “rotating” for the impeller and stationary for

the rest of the regions. The rotational velocity and the axis of rotation were also defined in this section.

The analyses conducted in this project required input of a turbulence model to close the governing equations, namely Reynolds-averaged Navier-Stokes equations (RANS) [48]. RANS equations were employed in the analyses since the computational effort required to solve the direct numerical simulation of Navier-Stokes equations were beyond the capability of utilized computer power. The turbulence model in analyses was set to k-ω based Shear Stress Transport (SST) which was proven to be successful by other researchers as mentioned in literature review chapter.

The boundaries were adjusted as mass flow rate at the inlet and zero static pressure at the outlet. Mass flow rate was set to flow rate of the desired simulation condition. Another boundary condition was the upper wall of the impeller fluid surface which was adjusted as a counter-rotating wall so that the fluid within the axial gap resolved more accurately as suggested by ANSYS Help [47].

Three interfaces were defined between the rotating and stationary regions due to the complex nature of the joint face (Figure 10).

a) Impeller (lower end of washout holes) → Volute
b) Impeller (region between blades) → Volute
c) Inlet → Impeller

The designs with no washout holes did only have the b and c interfaces. The interface was modeled with “frozen rotor” which handled the changes in frame of reference and pitch.

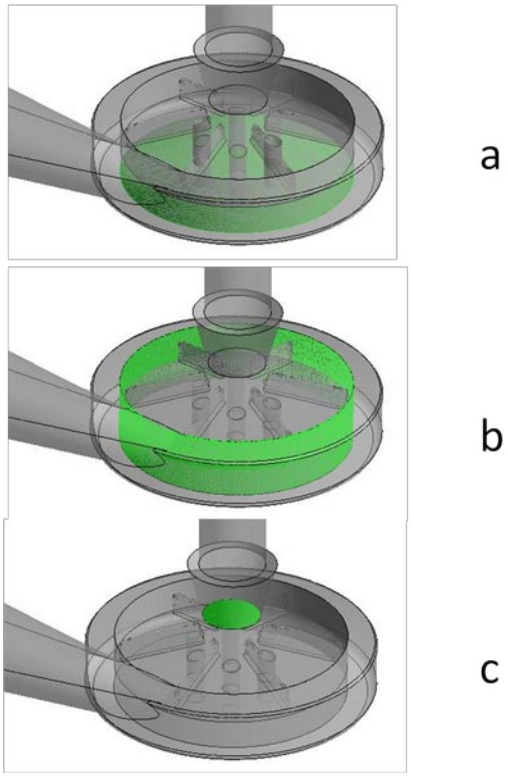

Figure 10: Interfaces between rotating and stationary regions

Next step was defining the parameters under "solver control" which governed the solution. The analyses progressed in an iterative manner and the maximum number of iterations was set to 3000. Timescale was adjusted to one-320th of a revolution time. The iterative solution was stopped if the convergence criteria, which were adjusted over the value of root mean square (RMS) residuals, were met. The target value for RMS residuals was set to 10^{-4}. In the "output control" section, the pressure of a point at the inlet of the pump was defined to be monitored so that the hydraulic performance values were viewed during the simulations.

After completing the definition of the solution, a definition file with the *.def* extension was created. CFX-Solver used definition file to account for the details of the

geometry and simulation details. Introducing the definition file to the CFX-Solver, the analyses started to solve the RANS equations. Meanwhile, RMS residuals and pre-defined monitoring points were depicted on the screen. The monitor screening the pressure at the inlet after completion of the analysis is shown in Figure 11. Analyses were finished either after reaching the maximum number of iterations or RMS residuals. The time spent for solution was around 40 hours.

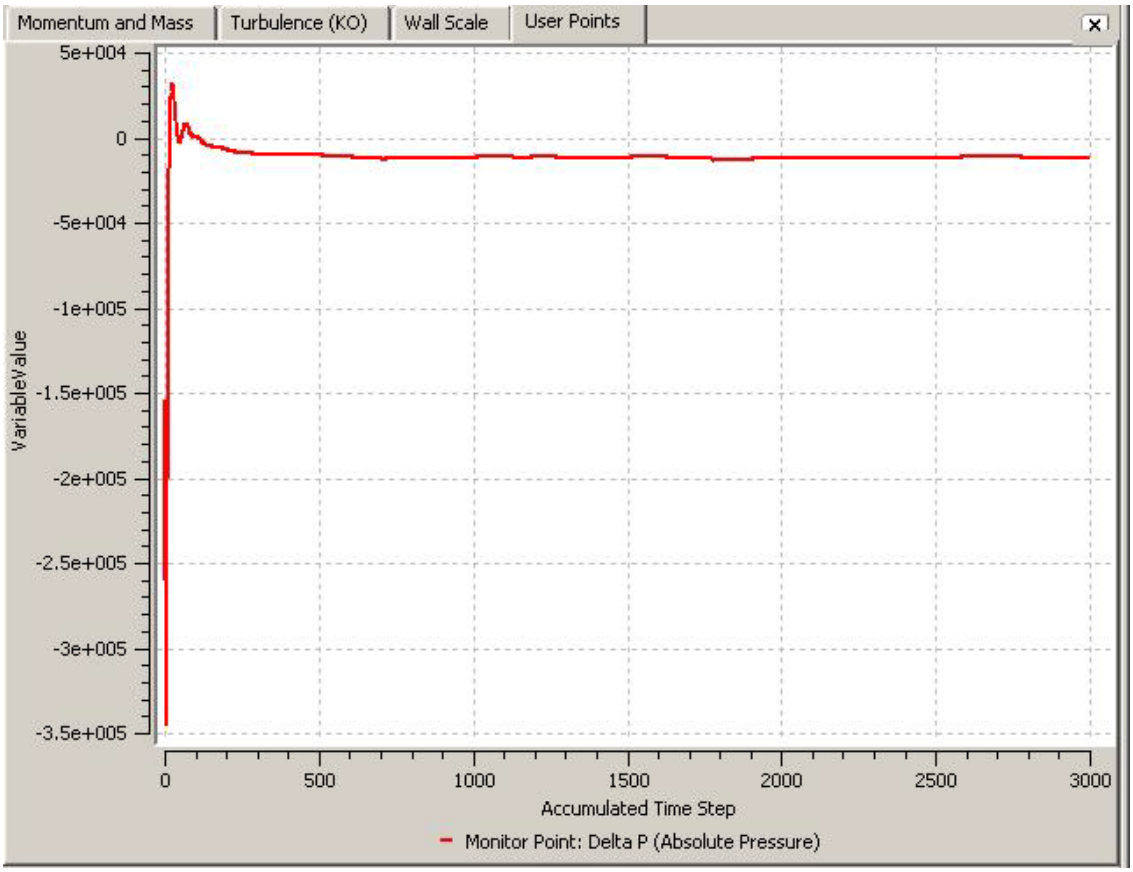

Figure 11: CFX-Solver screen monitoring the pressure at the inlet

Ending up with a result in CFX-Solver, Advanced CFD module provided excellent post-processing tools. Pressure distribution could easily be viewed by contour plotting the variable as depicted in Figure 12.

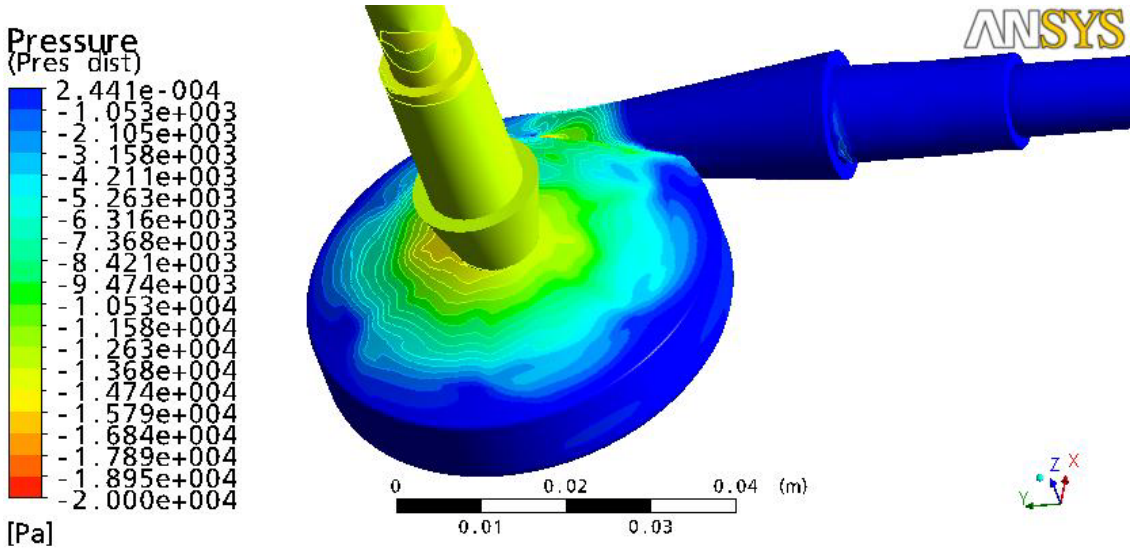

Figure 12: Pressure distribution view in Advanced CFD post-processing

Post-processing tools allowed definition of a new variable which was calculated with the pre-calculated ones as results of the analyses. By utilizing this property, shear stress calculations in the pumps, which suggested an idea about hemolytic performance, were conducted. In doing so, shear stress calculations were realized according to the Equation 1.

$$S_{scalar} = \frac{1}{\sqrt{3}}\sqrt{\sigma_{ii}^2 + \sigma_{jj}^2 + \sigma_{kk}^2 - \sigma_{ii}\sigma_{jj} - \sigma_{jj}\sigma_{kk} - \sigma_{kk}\sigma_{ii} + 3\left(\sigma_{ij}^2 + \sigma_{jk}^2 + \sigma_{ki}^2\right)} \qquad 1$$

The shear stress (σ_{ij}) was summation of molecular stress (η_{ij}) and Reynolds stress (τ_{ij}) as in Equation 2.

$$\boldsymbol{\sigma_{ij}} = \boldsymbol{\eta_{ij}} + \boldsymbol{\tau_{ij}} \quad \textbf{2}$$

$$\boldsymbol{\eta_{ij}} = \boldsymbol{\mu}\left(\frac{\partial \boldsymbol{u_i}}{\partial \boldsymbol{x_j}} + \frac{\partial \boldsymbol{u_j}}{\partial \boldsymbol{x_i}}\right) \quad \textbf{3}$$

Molecular stress is equal to the multiplication of the viscosity and the mean velocity gradients as in Equation 3 and Reynolds stress as follows:

$$\boldsymbol{\tau_{ij}} = -\frac{2}{3}\boldsymbol{\rho k \delta_{ij}} + \boldsymbol{\mu_t}\left(\frac{\partial \boldsymbol{u_i}}{\partial \boldsymbol{x_j}} + \frac{\partial \boldsymbol{u_j}}{\partial \boldsymbol{x_i}}\right) \quad \textbf{4}$$

where μ, μ_t, ρ, k, δ are viscosity, turbulent viscosity, density, turbulence kinetic energy and Kronecker's delta, in order. Since the input variables were already calculated as results of the CFD analyses, calculation of the shear stress was possible by writing an expression and generating a variable within the post-processing tool of ANSYS Workbench Advanced CFD module. Later, the generated shear stress variable could also be viewed by contour plots (Figure 13).

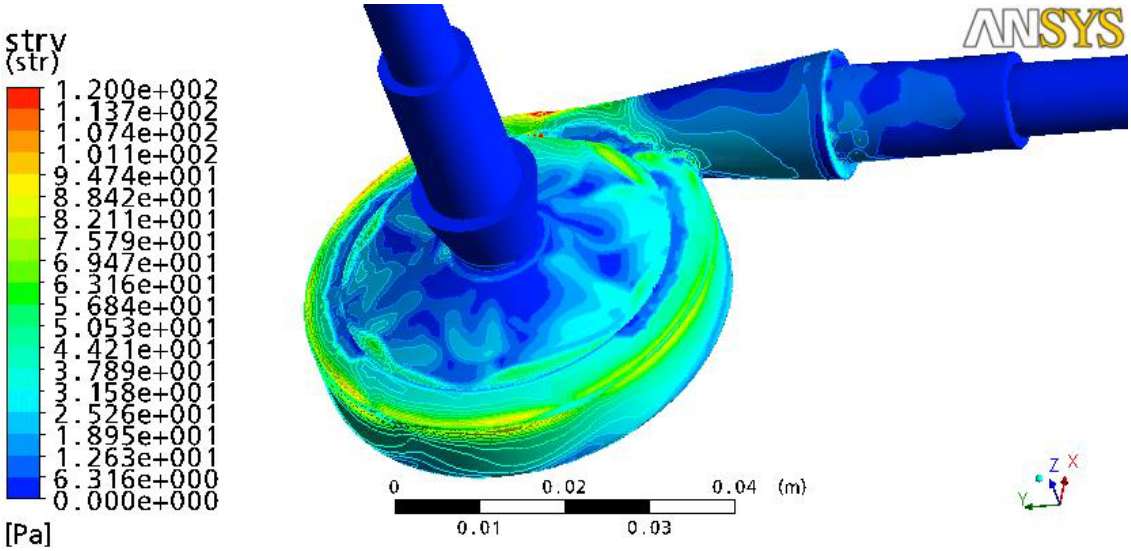

Figure 13: Stress distribution view in Advanced CFD post-processing

Velocity vectors could also be viewed with the post-processing tools. In the application, plotting was adjusted to be generated of vectors and the variable was chosen as velocity. An instance of velocity vectors view is depicted in Figure 14. The views of velocity vectors provided idea about the flow behavior within the pump such as the direction of the flow. Flow behaviors in more specific regions were observed as will be presented in the results chapter.

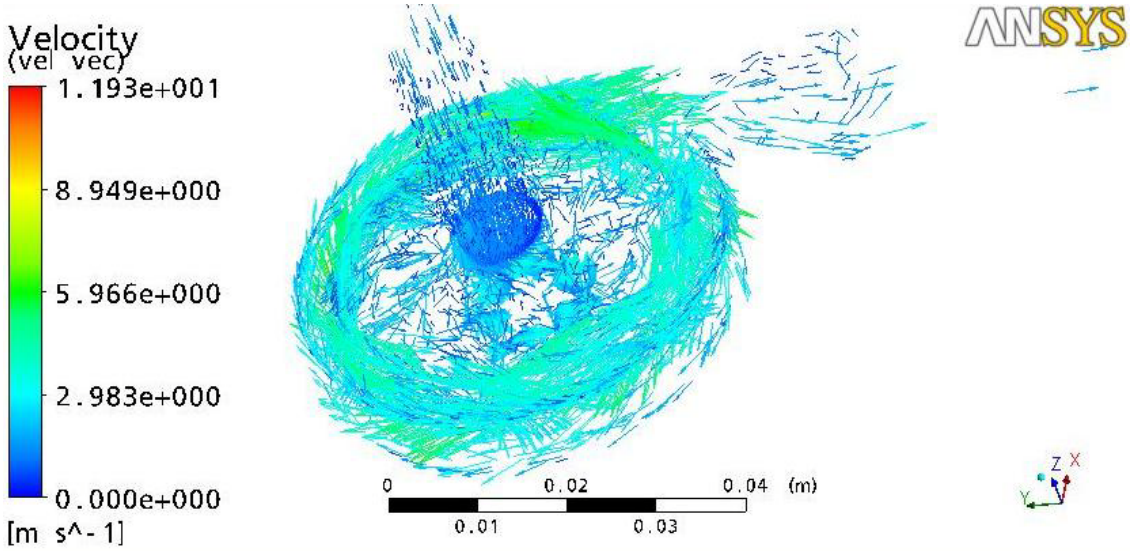

Figure 14: Velocity vectors view in Advanced CFD post-processing

3.3. Manufacturing

Manufacturing phase in the development of HTC started with the Computer Aided Manufacturing (CAM) of the designed part. CAM was followed by manufacturing of the pump in Computer Numerical Control (CNC) machine. Finally, the assembly of the pump was realized.

CAM was utilized in order to generate the G-codes for manufacturing and simulate the manufacturing process. G-codes were composed of coordinates and paths that the tool in CNC machine machined and followed, respectively. In CAM, geometries of the work piece, cut regions and tool were introduced initially. Besides, the tool path and cutting parameters were defined so that the software generated the G-codes. In Figure 15, orange, magenta and blue colored lines represent the work piece, cut region and tool path, in order. The simulation of the manufacturing process with the generated tool path is demonstrated in Figure 16. The manufacturing process was realized in two steps: roughing and finishing. In many cases, a third-step called the semi-finishing was intercalated between the other two for the sake of easing the machining process by lightening the chip load in each step. In roughing, a stock between 500 μ and 1 mm was left to be processed in finishing.

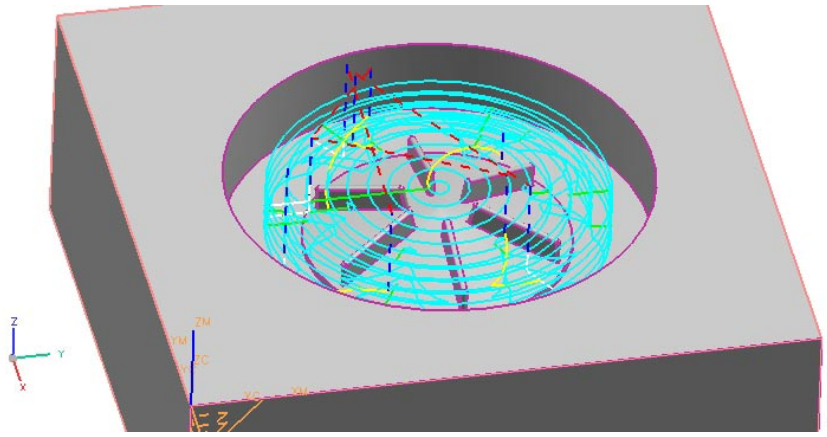

Figure 15: Tool path, work piece and cut region views in CAM

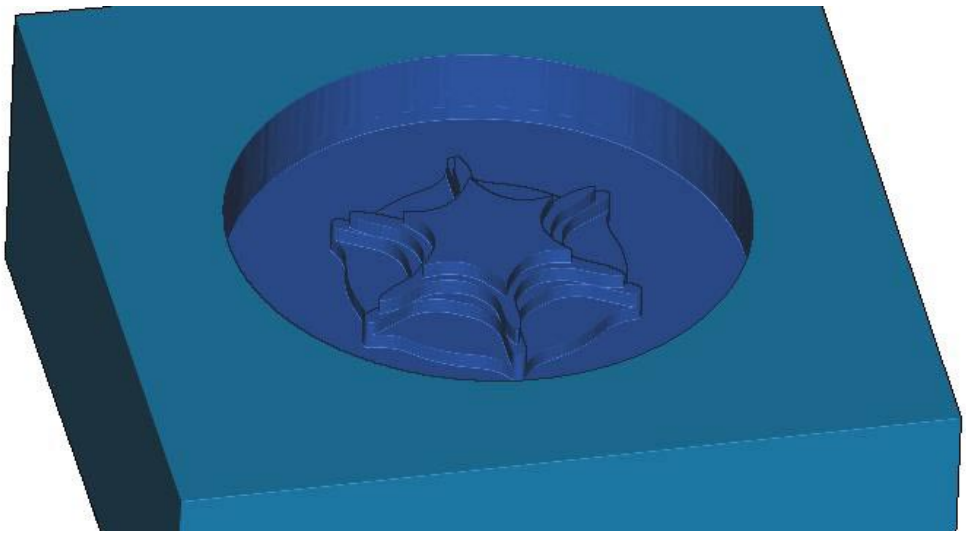

Figure 16: Simulation of the manufacturing process in CAM software

The G-codes were then exported from the CAM tool of Unigraphics and tested in another software, called CIMCO, for verification in order to avoid any software malpractice of the first CAM tool. Double-checked G-codes were carried to the CNC machine for manufacturing. The CNC machine employed in development of HTC was a high precision and high speed one, namely Mazak FJV-200 UHS Vertical Machining Center (Figure 17). The machine had a maximum spindle speed of 25000 rpm and ±2.5 micron sensitivity.

Figure 17: Mazak FJV-200 UHS Vertical Machining Center

The pumps were manufactured in three parts: lower cap, impeller and upper cap. All three parts were extracted from 95x95x40 mm blocks made of Poly Methyl Methacrylate (PMMA). In manufacturing the parts, ball-end mill tool in diameter of 3 mm and end-mill tools in diameters of 5 and 12 mm were used.

Completing the manufacturing of three parts, initially, magnets and bearing were embedded at the back-side of the impeller. In order to get tight fits of magnets and bearings, holes were manufactured 30 and 40 μ smaller than the dimensions of magnets and bearing, respectively. The impeller was then mounted to the lower cap through the bearing in the impeller and shaft on the lower cap. Silicon was applied on the surface of the lower cap that faces the upper cap so that the pump was sealed. Next, the upper cap was assembled to the lower cap with the aid of bolts and nuts. Last, the inlet and outlet holes were screwed and then the tube fittings were connected to the pump. The whole

manufacturing process including the CAM, labor in CNC machine and assembly required approximately 30-40 hours of work.

3.4. Experimentation

Experiments were conducted in order to measure the hydraulic performance of the manufactured pump. Initially, the pump was integrated into the experimental setup via the tube fittings that were already assembled to the pump. The experimental setup was consisted of reservoir, two pressure sensors, pump, motor and its driver, three power supplies, a DAQ card and computer (Figure 18).

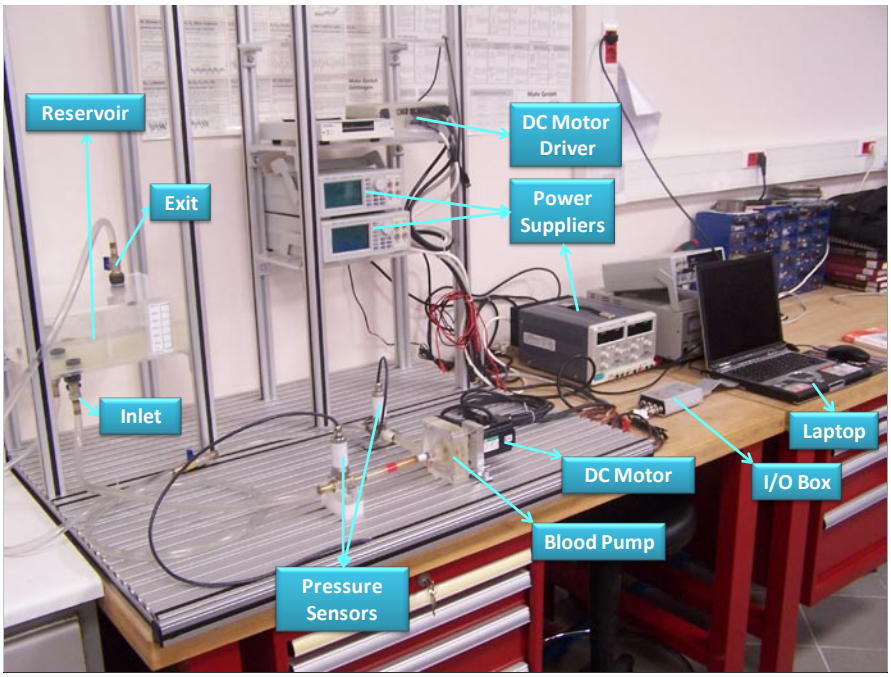

Figure 18: Experimental setup

One of the power supplies were employed to provide power to the motor while another one was used for adjusting the speed of the motor. When the motor started to work, the circular disk mounted on to the shaft of the motor started to rotate which in turn actuated the impeller with magnetic coupling. As the impeller started to rotate, it started to suck fluid from the reservoir. Hence, the fluid sucked from the reservoir gained momentum in the pump and then flowed back to the reservoir. Meanwhile, the pressure sensors, which were powered with the third power supply, measured the pressure of the fluid at the inlet and outlet of the pump and sent signals to the DAQ card which delivered signals to the computer. The averages of the measured pressure data were taken in LabView software. The average inlet pressure was subtracted from the average outlet pressure to get the pressure generated by the pump. At the same time, flow rate was measured with a 1 L volume pot. The time lasted to fill the empty pot was recorded so that the results reflected the time spent for a 1 L flow. The valve at the discharge of the fluid to the reservoir was throttled in order to vary the flow rate. In addition, the rotational speed of the pump was also changed. Thus, the performance data of the pump (pressure difference) at different operating conditions (flow rate, speed) were recorded.

The data points each representing a particular pressure difference at a particular flow rate and speed were provided as inputs to the MATLAB software. The data points that belong to a rotational speed were curve-fitted by a second order polynomial. Each curve specific to one rotational speed were then represented on a plot x and y axis of which corresponded to flow rate and pressure difference, respectively (Figure 19). Following the procedure above, finally, the hydraulic performance of a pump was obtained.

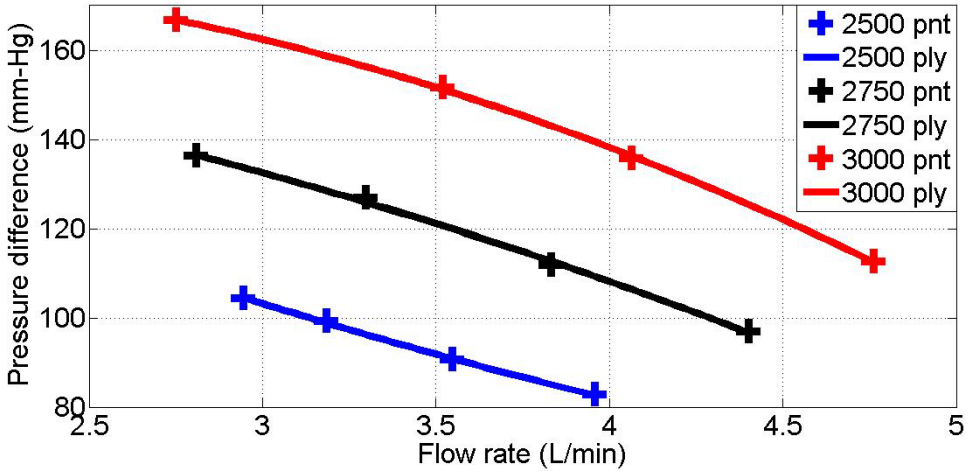

Figure 19: Experimental hydraulic performance graph of a pump

3.5. Design tools

As mentioned in the introduction chapter, design of Centrifugal Blood Pump (CBP) was the main consideration of the presented work. Design phase of the development of HTC mainly composed of determining the values of geometric design parameters of the pump. In determining the values of geometric design parameters, several design tools are available: one-dimensional (1-D) design procedure, CFD analyses and trial and error method. The applicability of the design tools described below were studied in detail by investigating their ability to assist the design by means of determining the values of geometric design parameters.

3.5.1. 1-D design procedure

1-D design procedure consisted of equations and charts to guide the designer. The designer inputs the desired pressure difference and flow rate at desired speed to the procedure and comes up with the values of geometric design parameters of the pump determined with the aid of equations and charts provided. The equations and charts presented by the procedure were emerged from the enormous empirical data collected for tens of years. While the design procedure was based on a simplified one-dimensional theory, the suggested values for geometric design parameters were quite certain. However, the tool was ultimately offered to provide an initial idea about the values of geometric design parameters due to its simple nature. While the procedure was introduced by a vast number of researchers, Gülich provided a good reference of the procedure in SI units in his book named "Centrifugal Pumps" [30]. Although the method provided a thorough procedure to calculate the values of all geometric design parameters, part of it will be presented in this section since the part serves enough material to be utilized in results chapter.

A designer attempted to use 1-D design procedure initially asked for the desired operating conditions. The desired operating conditions involved the desired pressure difference and flow rate at the desired rotational speed. The pressure difference and flow rate were easy to be figured out since the required operating conditions of CBPs were 5 L/min (0.833×10^{-4} m^3/s) flow rate against a pressure difference of 100 mm-Hg (1.3575 m head). The rotational speed was inputted with respect to the specifics of the design.

The first geometric design parameter to be determined in the procedure was the outer diameter of the impeller (d_2). Impeller outer diameter was calculated with Equation 5.

$$d_2 = \frac{60}{\pi N}\sqrt{\frac{2gH_{th}}{\psi_{opt}}} \quad \textbf{5}$$

where N was the rotational speed, H_{th} was the theoretical head and ψ_{opt} was the selected head coefficient. Among these variables, theoretical head of the pump was calculated as in Equation 6 with the desired head (H_{des}) and the estimated hydraulic efficiency (η_h) in hand.

$$H_{th} = H_{des}/\eta_h \quad \textbf{6}$$

The hydraulic efficiency was estimated through a chart (Figure 20) that requires the desired flow rate (Q_{des}) and specific speed (n_q).

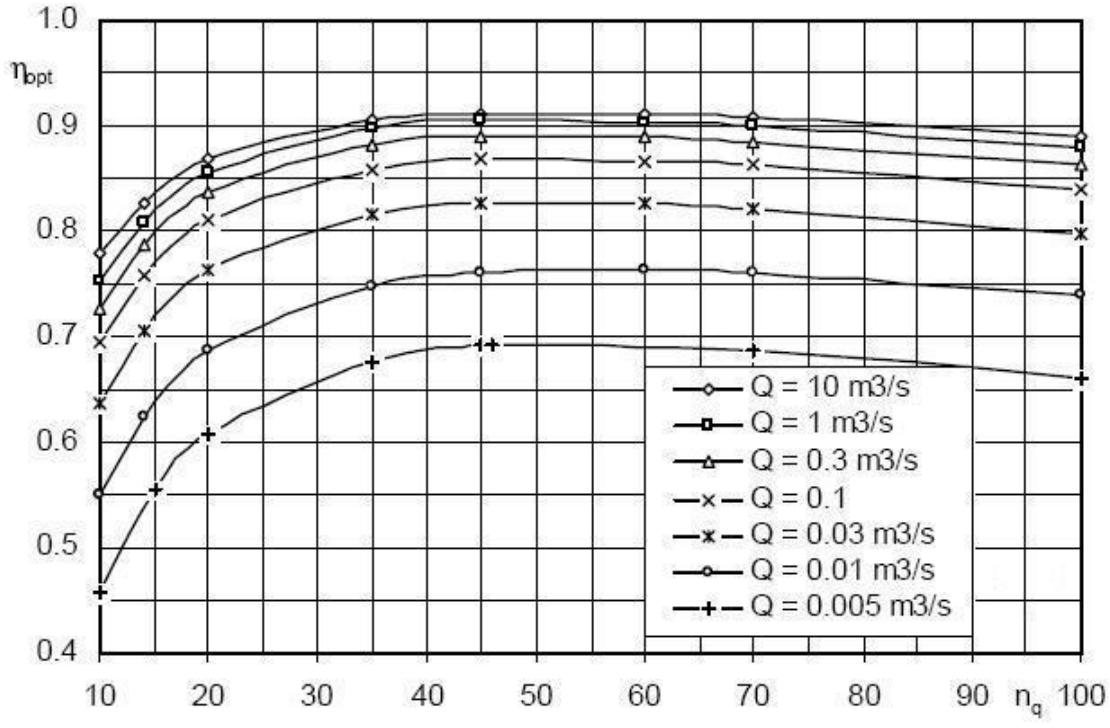

Figure 20: 1-D design procedure hydraulic efficiency chart

The specific speed was calculated with desired flow rate, desired rotational speed and head as in Equation 7.

$$n_q = N \frac{\sqrt{Q_{des}}}{H_{des}^{0.75}} \quad (7)$$

The theoretical head and the impeller's outer diameter could easily be calculated, in order, after the prediction of the hydraulic efficiency from the efficiency chart. The values of other geometric design parameters could also be calculated with equations and charts of the 1-D design procedure as well.

3.5.2. Computational Fluid Dynamics (CFD) analyses

CFD analyses were considered a design tool since it provided a virtual environment to test a particular design. In doing so, desired values could be assigned to the geometric design parameters and the resultant designs could be tested by CFD analyses. CFD analyses, more specifically, could be utilized in determining the values of geometric design parameters by assigning different values to a selected design control parameter and investigate the effects of different values in results of the analyses. In results of the analyses, hydraulic and hemolytic performances and regions prone to flow stagnation, thus thrombogenicity, could be examined. Hence, the optimum values of the desired geometric design parameters could be determined. The description of the tool with the procedure to use it was explained in CAE section of this chapter in detail. On the other hand, the procedure described in this section implies the role of the tool in determining the values of geometric design parameters.

The ability of CFD analyses to assist the design of CBPs in determining the values of geometric design parameters was investigated by comparing the success of the prediction of hydraulic performance of CFD analyses. The comparison was executed

over the hydraulic performances of two pumps predicted by CFD analyses and tested experimentally.

3.5.3. Trial and error method

Trial and error method utilized in design of CBPs by means of determining the values of geometric design parameters was composed of an initiation step and the main step. The initiation step included determining values of geometric design parameters based on the results of previous studies in the literature. In doing so, particular values those were proven to be superficial to the compared ones for a geometric design parameter in previous studies were taken into account. Combining knowledge from different sources, best values were assigned to the geometric design parameters of the considered design. The values of the geometric design parameters without any studies were issued about were estimated accordingly. One parameter was left as a control parameter to be studied in the second step.

The second step was the trial and error part that different values of the geometric design control parameter were studied. The step progressed in an iterative manner where the value of the control parameter was set with respect to the affinity laws after the first iteration. Affinity laws suggested proportions among operating conditions and geometric design parameters of the pump. For instance, rotational speed of the pump could be increased with a reduction in the value of the impeller outer diameter. The affinity law utilized in this research was a relationship between the impeller outer diameter (d) and rotational speed (N) of the pump as is Equation 8. As the equation suggested, impeller outer diameter and rotational speed of the pump are inversely proportional.

$$\frac{d_1}{d_2} = \frac{N_2}{N_1} \quad \textbf{8}$$

Utilizing this tool, optimum value for the control parameter could be achieved in a few iterations. The iterations included the manufacturing and testing of the designed pump. The details of manufacturing and experimentation were described in sections of manufacturing and experimentation of this chapter, respectively.

Chapter 4: Results

This chapter presents the results of questioning the abilities of design tools to assist the design phase of Centrifugal Blood Pumps (CBPs). More specifically, the capabilities of the design tools in determining the values of geometric design parameters of a pump were investigated. The design tools investigated were one-dimensional (1-D) design procedure, Computational Fluid Dynamics (CFD) analyses and trial and error method. In addition, utilization of CFD analyses as a design tool by means of examining the flow behavior in post-processing was also presented. The methods to apply the design tools to the design of CBPs were described in materials and methods chapter in detail. The results emerged after application of these tools is the main consideration of this chapter.

4.1. 1-D design procedure

1-D design procedure was attempted to be utilized in design of CBPs by means of determining values of the geometric design parameters. The design tool, as explained in detail in materials and methods chapter, provides a thorough procedure to determine values of the geometric design parameters one by one. In the beginning of the procedure, user was asked to provide the desired operating point (conditions) of the pump which included the pressure difference, flow rate and rotational speed. The first two parameters were inputted as 100 mm-Hg and 5 L/min in accordance with the required operating condition of CBPs. The last parameter, the rotational speed of the pump, was inputted as 3000 rpm. Following the procedure, the first geometric design parameter to be decided was the impeller outer diameter. In order to determine the value of the impeller outer diameter the following procedure was followed:

- Determination of specific speed (Equation7)
- Determination of efficiency from the chart (Figure 20)
- Determination of theoretical head (Equation 6)
- Determination of impeller outer diameter (Equation 5)

To start with, specific speed was calculated with Equation 7 as in Equation 9:

$$n_q = 3000[\text{rpm}]\frac{\sqrt{0.000083[\text{m}^3/\text{s}]}}{(1.3575\ [\text{m}])^{0.75}} = 21.7323 \qquad 9$$

The next step was to determine the hydraulic efficiency of the design from the chart with the input parameters of dimensionless specific speed (21.7323 as calculated above) and flow rate of 5 L/min as $0.833\text{x}10^{-4}$ m^3/s. with the values in hand, the hydraulic efficiency of the pump could not be determined (Figure 21).

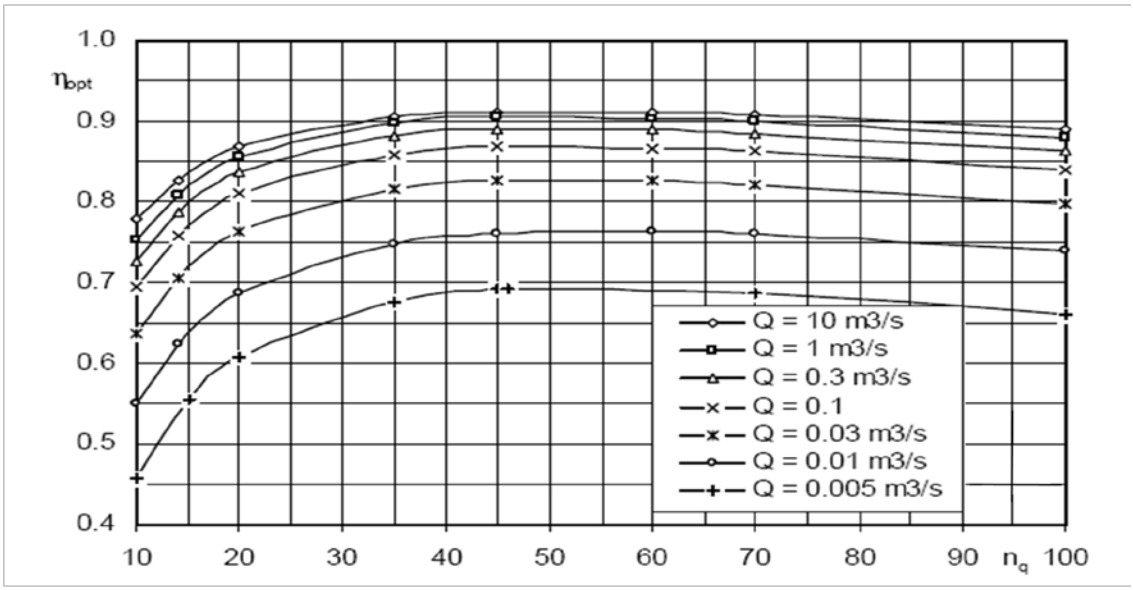

Figure 21: 1-D design procedure hydraulic efficiency chart range

The reason was obvious that the red circle on Figure 21 represented the operating point of CBPs which was not covered by the range of the hydraulic efficiency chart. The exception prevented the determination of the hydraulic efficiency and so the impeller outer diameter. 1-D design procedure was actually full of similar examples of being incapable of providing values for geometric design parameters of CBPs as demonstrated for impeller outer diameter in here. This way, 1-D design procedure was shown to be unsuitable to be employed in design of CBPs due to the valid ranges of the tool that did not cover CBPs. The details of the reasons regarding to the incapability of 1-D design reviewed will be discussed in discussion chapter in detail.

4.2. Computational Fluid Dynamics (CFD) analyses

The ability of CFD analyses to assist the design by means of determining the values of geometric design parameters was tested over the success of the prediction of experimentally measured hydraulic performance by the tool. The comparison was conducted over two pumps, namely Model 1 and Model 2. Model 1 and Model 2 were two distinctive designs with different values for almost every geometric design parameter. Design and manufacturing of Model 1 was work of a colleague as presented in his thesis [49] but the CFD simulations presented herein belong to this research. In contrast, all work related to Model 2 was a part of the presented thesis work.

Model 1 had 10.0 and 48.3 mm inlet and impeller inner diameter, respectively. The blade heights were from 5.0 mm at the leading edge decreasing down to 3.0 mm at the trailing edge with varying thickness narrowing through the edges. The back clearance was 100 microns while the radial and axial gaps were 100 and 175 microns, respectively. The impeller had 8 blades as shown in Figure 22.

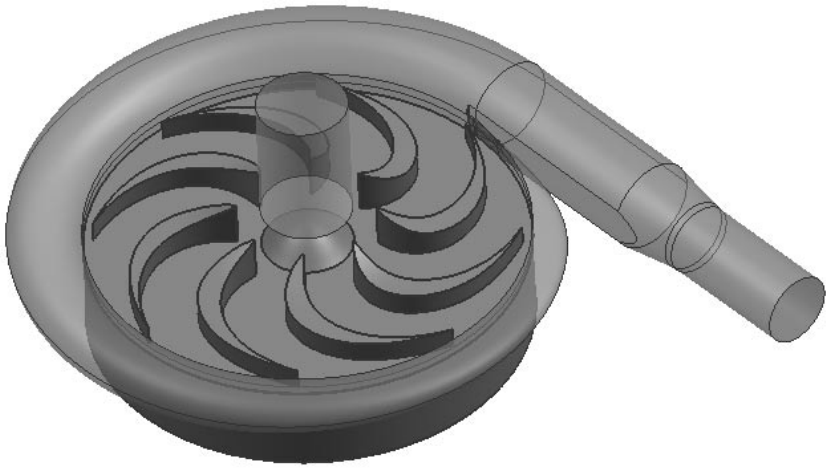

Figure 22: CAD view of Model 1

Model 2 was designed with 41 mm outer diameter, curved blades with angles of 60º at the leading and trailing edges. There were 6 blades with constant thickness and heights of 10 mm at the leading edge decreasing to 7.7 mm at the trailing edge. All gaps and the back clearance were set to 500 microns. The design was depicted in Figure 23.

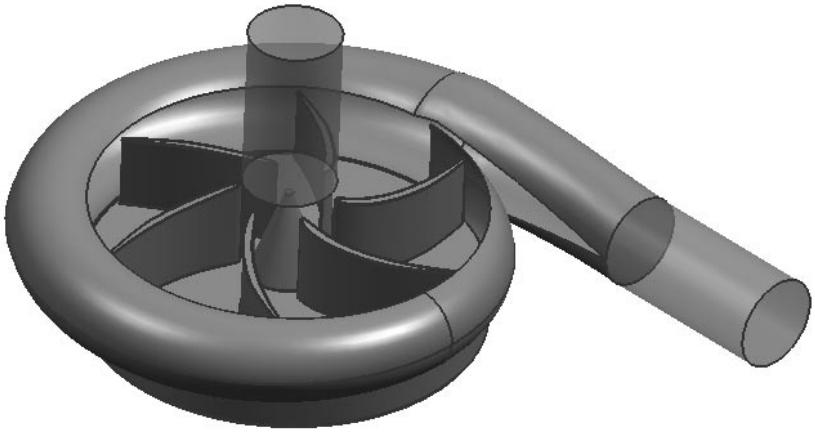

Figure 23: CAD view of Model 2

The models were meshed in CFX-Mesh module of Advanced CFD with the method described in Computer Aided Engineering (CAE) section of materials and methods chapter. Model 1 had 1249 K tetrahedrons, 533 K prisms and 27 K pyramids in the mesh. Model 2 was meshed with 985 K tetrahedrons, 437 K prisms and 20 K pyramids. The meshes of the impellers of Model 1 are depicted in Figure 24, Figure 25 and Figure 26 while the ones of Model 2 were in Figure 27, Figure 28 and Figure 29.

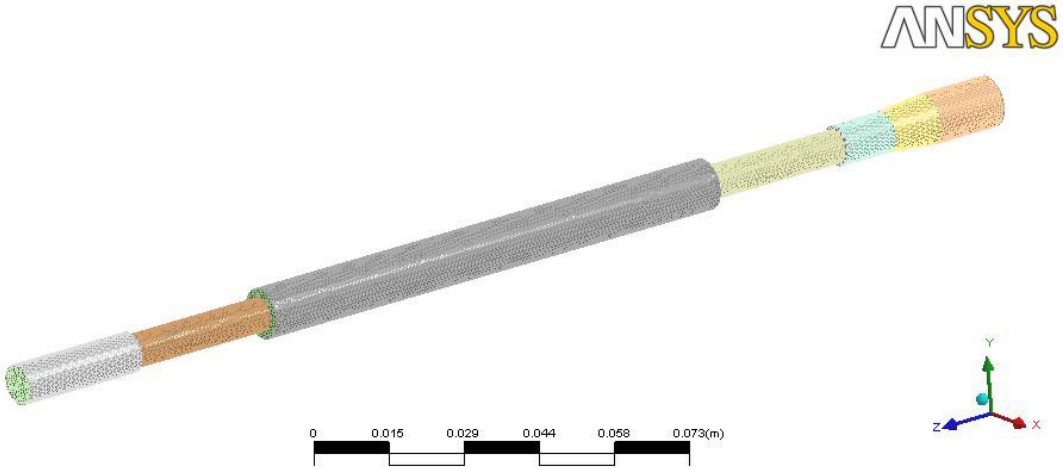

Figure 24: Inlet mesh of Model 1

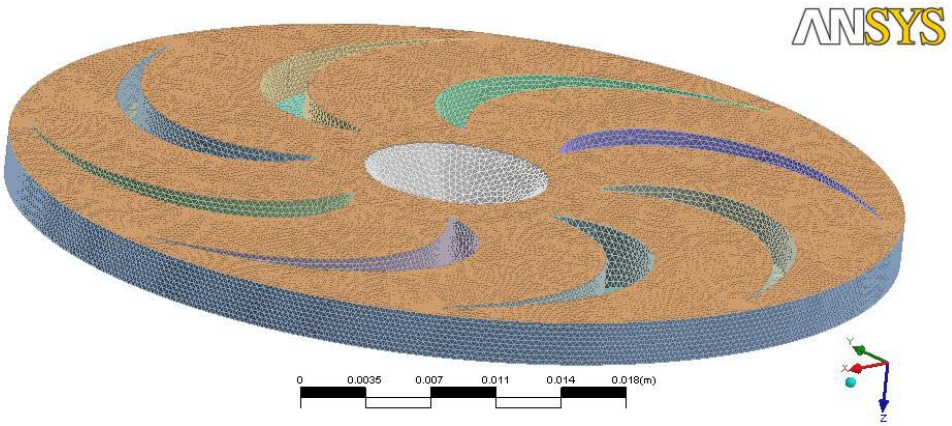

Figure 25: Impeller mesh of Model 1

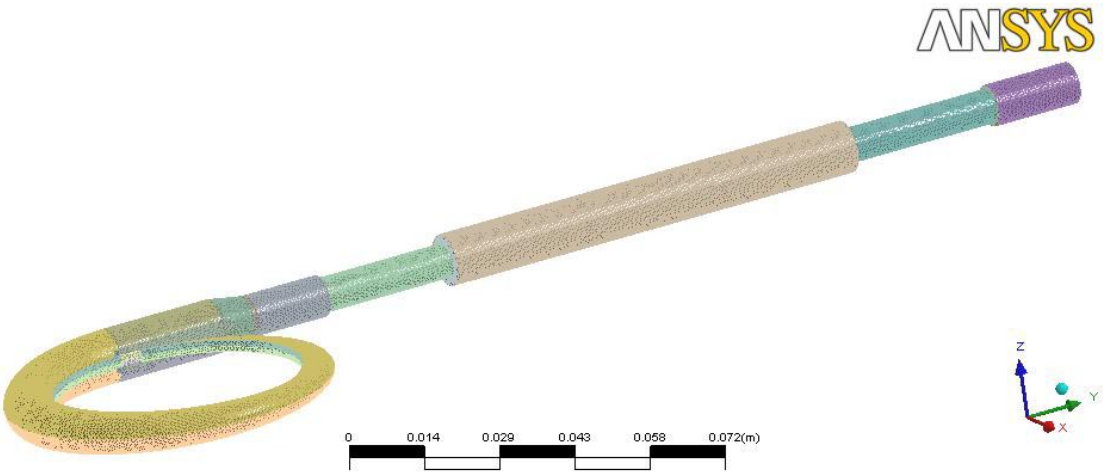

Figure 26: Volute and outlet mesh of Model 1

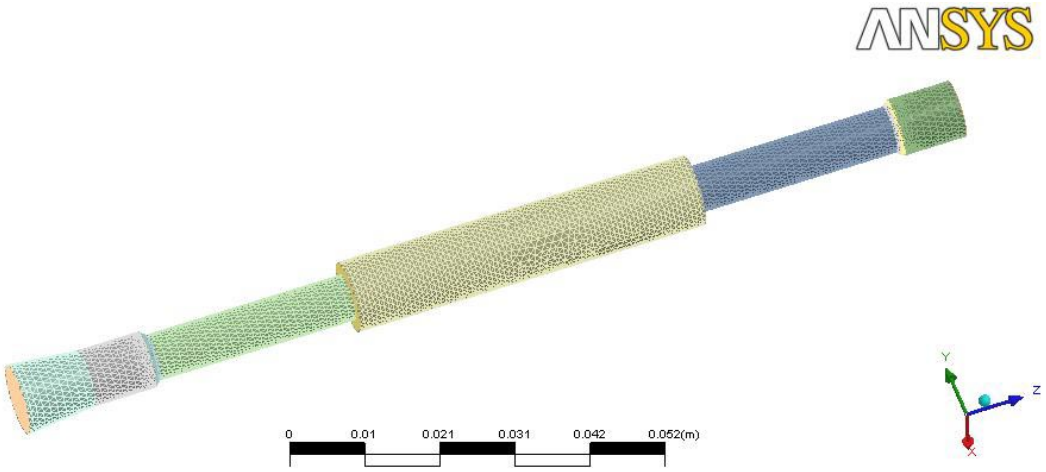

Figure 27: Inlet mesh of Model 2

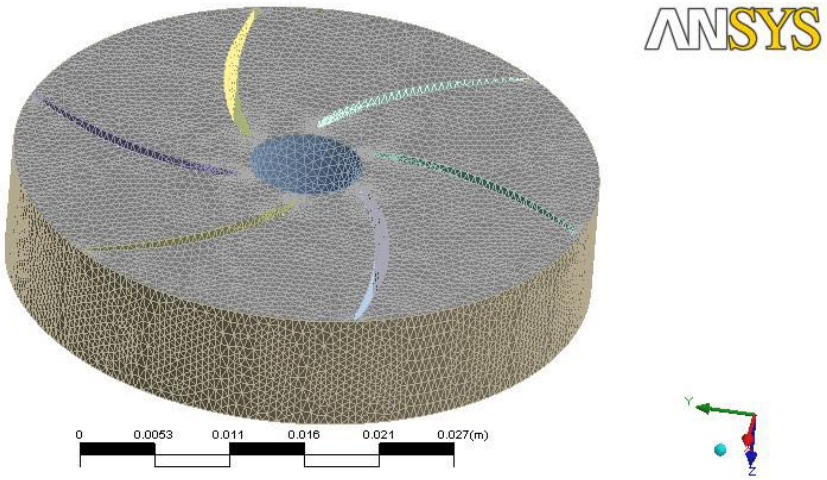

Figure 28: Impeller mesh of Model 2

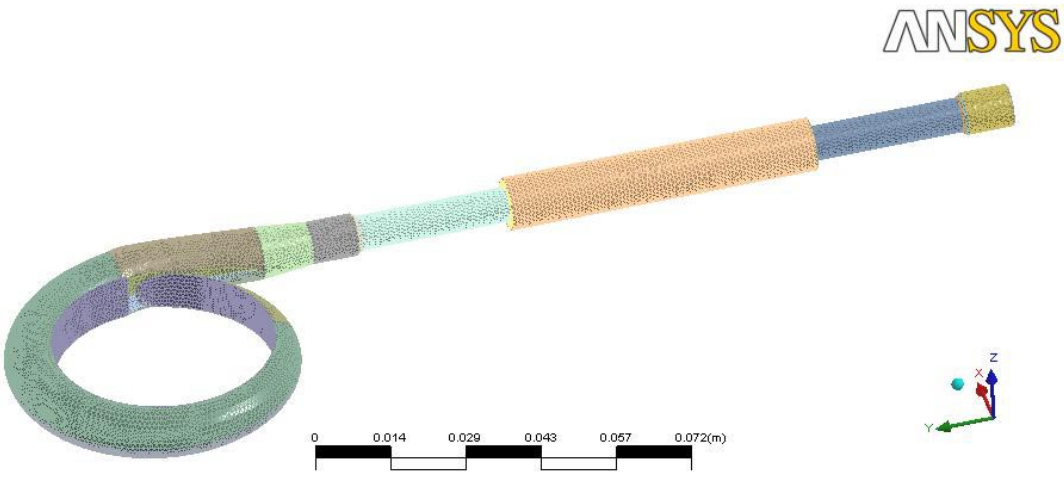

Figure 29: Volute and outlet mesh of Model 2

CFD analysis was executed for Model 1 at the performance point of 5.3 L/min flow rate against a pressure difference of 120 mm-Hg at a rotational speed of 3000 rpm. The simulation point for Model 2 was 4.98 L/min against a pressure difference of 108.84

mm-Hg at rotational speed of 3000 rpm. Water was introduced as the medium in the analyses since it was the type of fluid used in the experiments. SST was employed as the turbulence model. Convergence criteria were set to a value of 10^{-4} for RMS residuals and 5000 iterations. CFD analyses were converged at the iteration of 917 for Model 1 (Figure 30) while the RMS residuals were decreased down to $9x10^{-4}$ at most after the 5000 iteration for Model 2 (Figure 31).

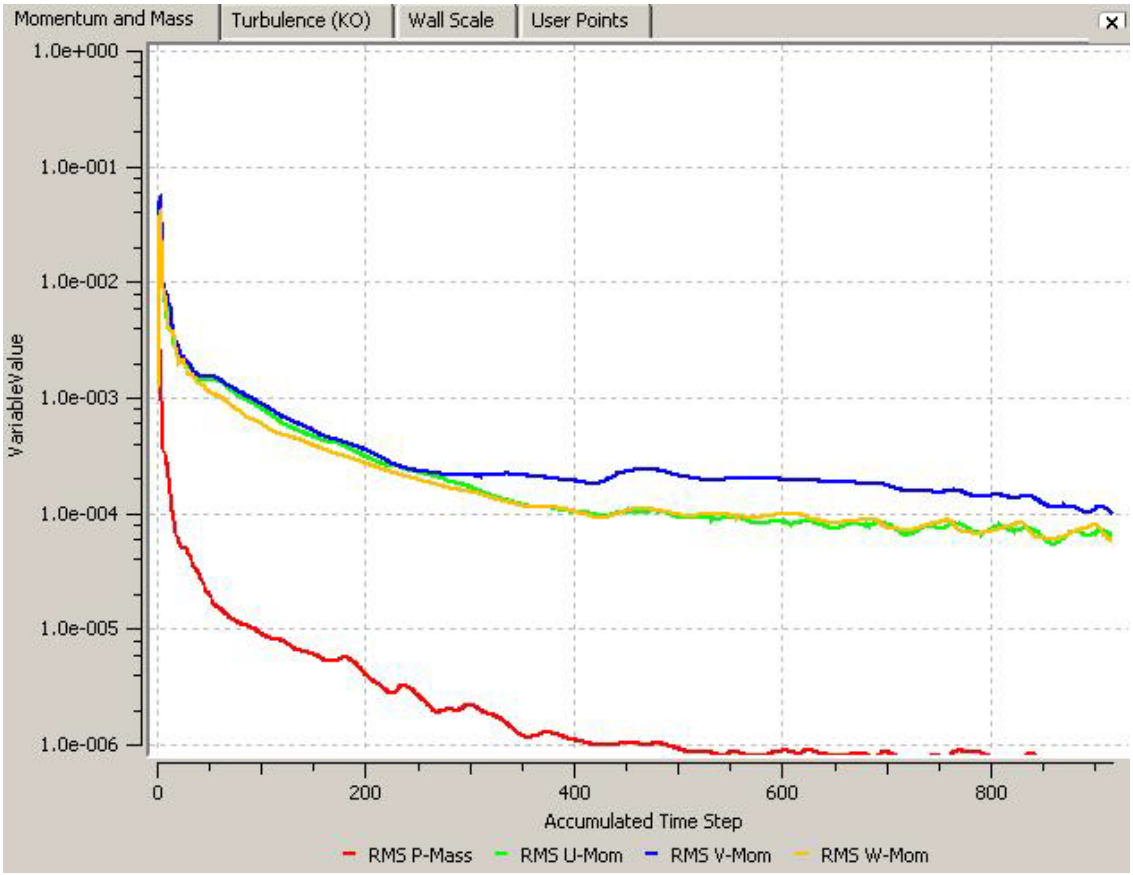

Figure 30: Convergence of Model 1 CFD analyses

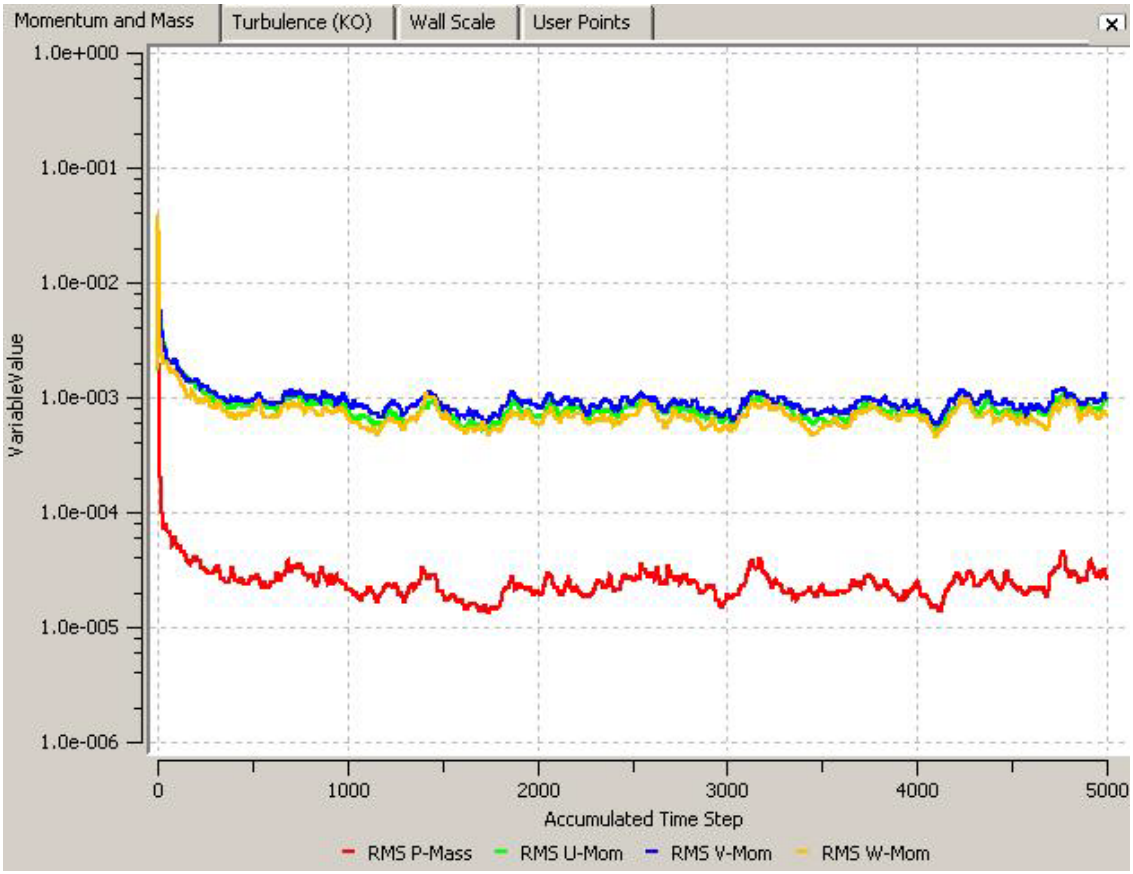

Figure 31: Convergence of Model 2 CFD analyses

Experimental results, predictions of CFD analyses and the error rates of the CFD analyses at the considered operating point were presented in (Table 5).

Table 5: Experimental and CFD results for Model 1 and Model 2

Pump name	**Model 1**	**Model 2**
Experimental results (mm-Hg)	120	108.84
Predictions of CFD analyses (mm-Hg)	137.54	175.32
Error rate of CFD analyses (%)	14.6	61

Although the simulation details were the same and operating points were kept close, the prediction ability of CFD analyses were quite different for the pumps. The results suggested that CFD analyses did predict the performance for one pump but failed for the other. This way, it was shown that CFD analyses could not predict the performance of many designs. Hence, foreseeing the performance of a CBP before manufacturing and adjusting the values of the geometric design parameters respectively was rendered impossible. That is why CFD analyses were proven to be useless to determine values of the geometric design parameters prior to manufacturing. Consequently, CFD analyses could not be used alone in the design phase as a design assisting tool by means of determining values of the geometric design parameters. The reasons of failure as well as the advantageous aspects of CFD analyses will be covered in discussion chapter.

4.3. Trial and error method

Trial and error method composed of an initiation part in that values of the geometric design parameters were determined following previous studies of the literature and a trial and error part in which the value of the control parameter left in the first part was determined after a few iterations of designs whose were experimentally evaluated. In doing so, Model 3 was designed with values of the geometric design parameters determined by inspiration from particular studies in the literature (Figure 32). The impeller was shaped with 6 radial straight vanes [29], radial and axial gaps were configured as 5.0 mm [17] and 1.5 mm [19], respectively. Back clearance between the back of the impeller and the housing was determined to be 250 microns in order to impede the backflow to this clearance [9]. Outlet port position was adjusted accordingly in order to impede the blockage of the outlet port by the vanes [27]. Washout holes were introduced into the design of the impeller so that the flow stagnation on the back side of the impeller was prevented [21]. The pump was designed

as volute-less where the cylindrical hole in the lower cap acts like a volute. The exploded view of Model 3 in three parts with magnets and bearing included is depicted in Figure 33.

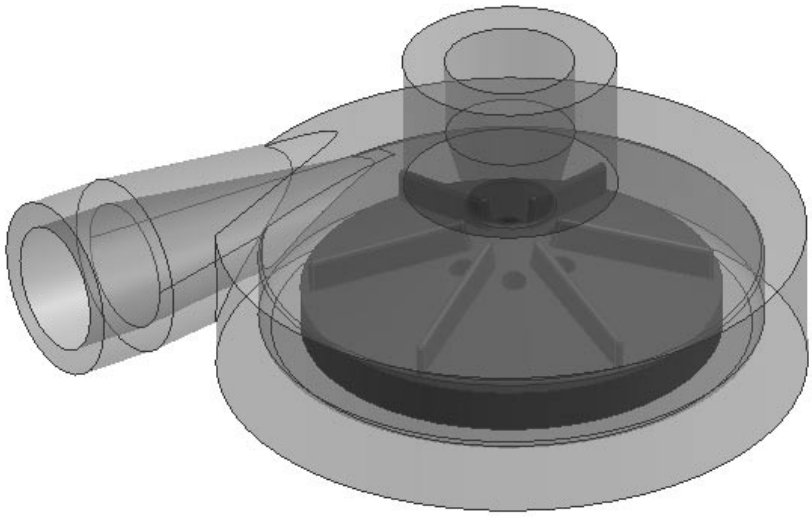

Figure 32: Cad view of Model 3

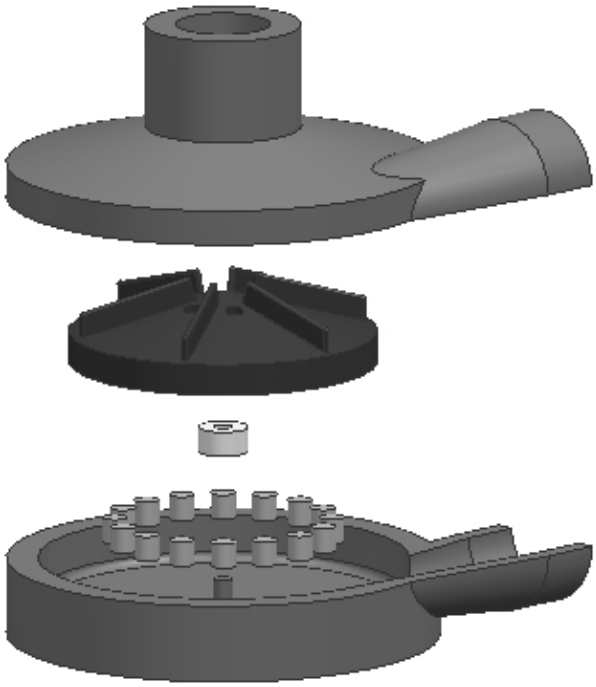

Figure 33: Exploded CAD view of Model 3

Impeller outer diameter was left as the geometric design control parameter. The initial value of the control parameter was set to 50 mm in an overestimated manner since the previous experience suggested that the minimum obtainable value of impeller outer diameter could be smaller than 50 mm. The pump was tested experimentally with the blood analogous as the medium. The results revealed that the desired operating condition, 5 L/min flow rate against a pressure difference of 100 mm-Hg, was achieved at a rotational speed of 2300 rpm by interpolating the data presented in Figure 34. Maximum possible flow rate of Model 3 was found as 8.05 L/min against a pressure difference of 80 mm-Hg at 2750 rpm rotational speed.

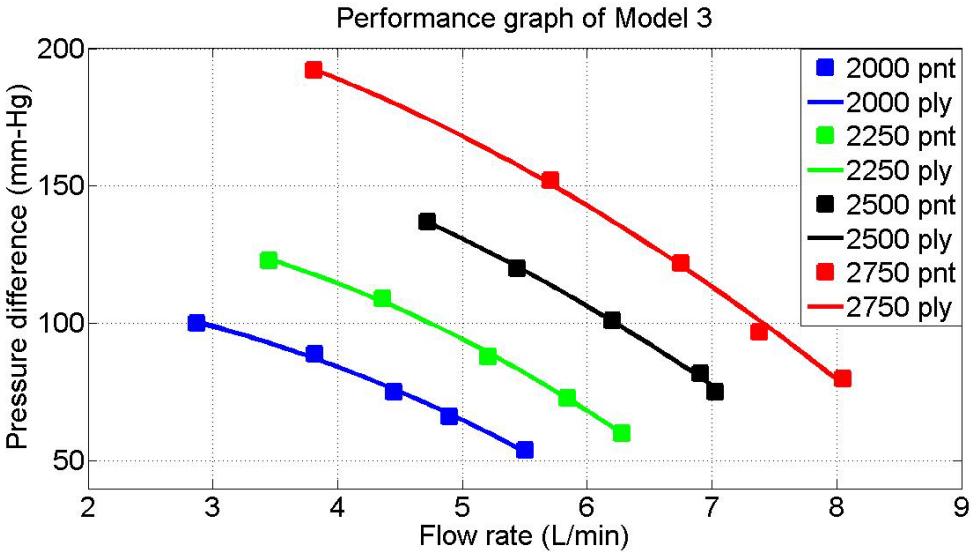

Figure 34: Experimental performance of Model 3

Based on the results of Model 3, impeller outer diameter of the next pump was determined with the aid of affinity laws. In this respect, Equation 8 was issued with input parameters:

d_1: 50 mm

N_1: 2300 rpm

N_2: 3000 rpm

Desired rotational speed of the second pump (N_2) was set at 3000 rpm since the value was the maximum speed of the motor used in experimental tests. Besides, 3000 rpm was considerably a high level speed for CBPs. The affinity laws suggested a value of 38.3 mm impeller outer diameter for the next pump as in Equation 10:

$$\boldsymbol{d_2 = d_1 \frac{N_1}{N_2} = 50[mm] \frac{2300\ [rpm]}{3000\ [rpm]} = 38.3\ [mm]} \qquad \textbf{10}$$

The impeller outer diameter of the second pump, namely Model 4, was determined as 40 mm in order to be safe. Values of the rest of the parameters other than the impeller outer diameter were kept same as the values set for Model 3. The normal and exploited CAD views of Model 4 were same as the ones presented for Model 3 in Figure 32 and Figure 33 with only one difference in impeller outer diameter which was trimmed to 40 mm from 50 mm. Model 4 was tested experimentally from which the results depicted in Figure 35 were derived.

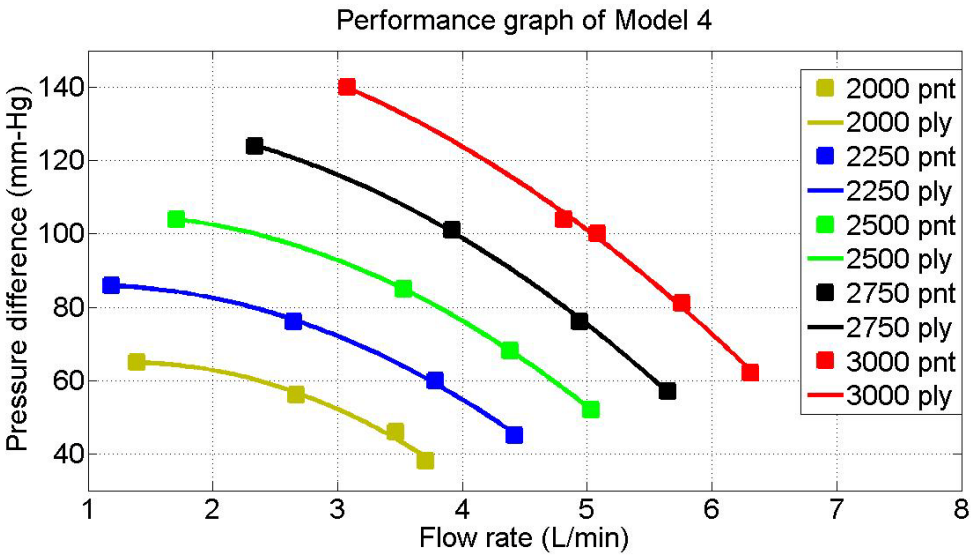

Figure 35: Experimental performance of Model 4

The pump achieved to desired operating condition at exactly 3000 rpm and maximum possible flow rate of the pump was 6.31 L/min against a pressure difference of 62 mm-Hg at 3000 rpm. The results proved that the design tool of trial and error method initiated with an inspiration from the previous studies was applicable to determine the values of geometric design parameters and come up with a CBP design. Using the tool, control parameters and values assigned to them could be varied so that effects of different values of geometric design parameters could be identified. This

way, the design of a desired CBP could be handled. The indications of the result as well as the pros and cons of the tool will be discussed in discussion chapter.

The trial and error method introduced in this research continued with use of CFD analyses in investigating the pump's inner flow. However, before use of CFD analyses, the correctness of the tool was verified. More specifically, in order to utilize the advantages of CFD analyses, the tool was validated by successful prediction of experimentally measured hydraulic performance results. CFD analyses were executed at desired operating conditions experimental results of which was revealed as 5 L/min flow rate against a pressure difference of 100 mm-Hg at a rotational speed of 3000 rpm. In order to realize the CFD analyses, fluidic geometries of Model 4 were meshed in CFX-Mesh in three parts as inlet (Figure 36), impeller (Figure 37) and outlet which included the volute (Figure 38).

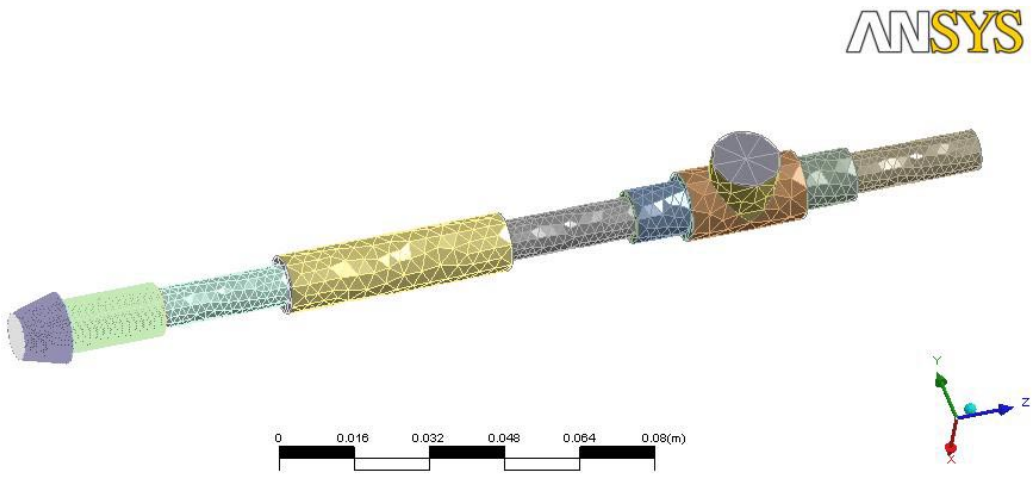

Figure 36: Inlet mesh of Model 4

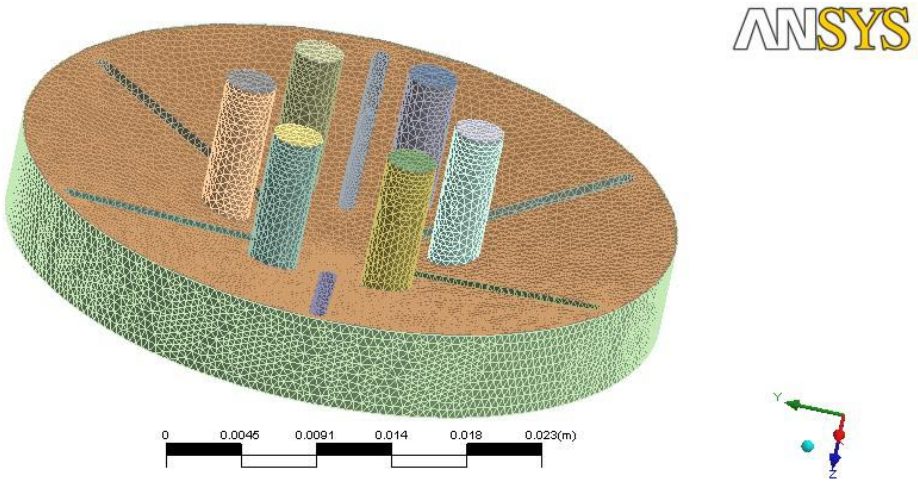

Figure 37: Impeller mesh of Model 4

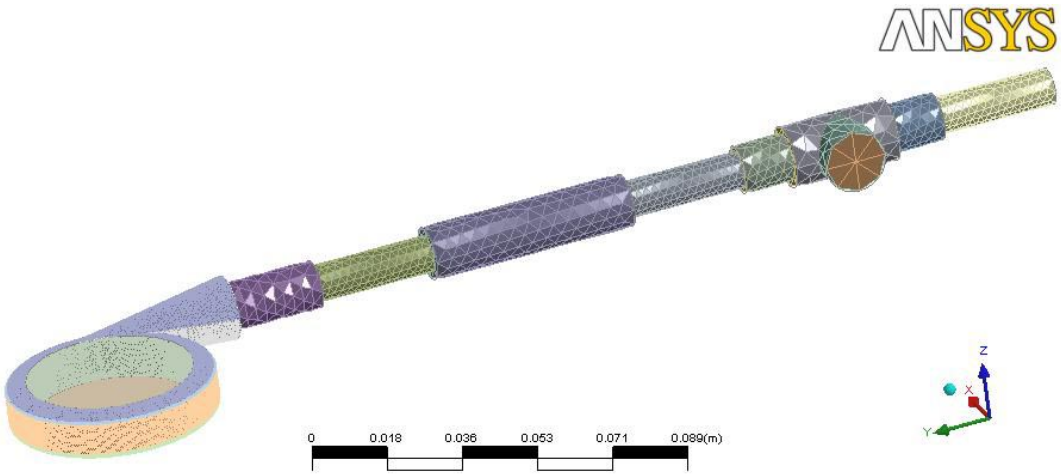

Figure 38: Volute and outlet mesh of Model 4

The mesh was condensed in inlet and outlet regions those were close to impeller and volute, respectively. The meshes in three regions contained number of elements as presented in Table 6.

Table 6: Number of elements in mesh of Model 4

Region	Inlet	Impeller	Volute & Outlet
Tetrahedrons	70 K	399 K	606 K
Prisms	14 K	186 K	210 K
Pyramids	-	1 K	5 K
Total	84 K	586 K	821 K

The analyses were run for convergence to either drop of RMS residuals to 10^{-4} or a maximum iteration of 3000. As a result, RMS values were at most converged down to 10^{-3} so that the analyses were terminated at iteration of 3000. However, the pressure difference at the considered point was predicted as 90.5 mm-Hg where the experimental one was 100 mm-Hg. The results, thus, concluded up with an error rate of 9.5 % which was considered well with respect to the ability of the tool. It was stated that CFD analyses was validated with the presented results so that the post-processing tools could be utilized comfortably with an error rate of at most 10 %.

In post-processing tools, plenty of information was gathered at the operating conditions of Model 4. In this respect, pressure distribution (Figure 39 and Figure 40), velocity vectors within the whole pump (Figure 41 and Figure 42) and at the washout holes (Figure 43), shear stress distribution (Figure 44 and Figure 45) and streamlines (Figure 46 and Figure 47) were reviewed.

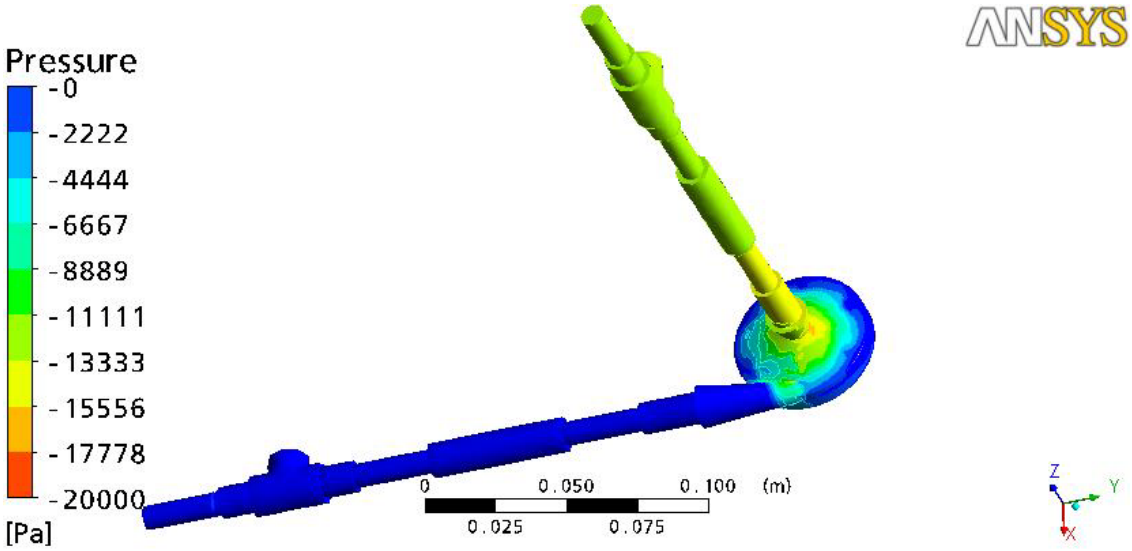

Figure 39: Pressure distribution of Model 4

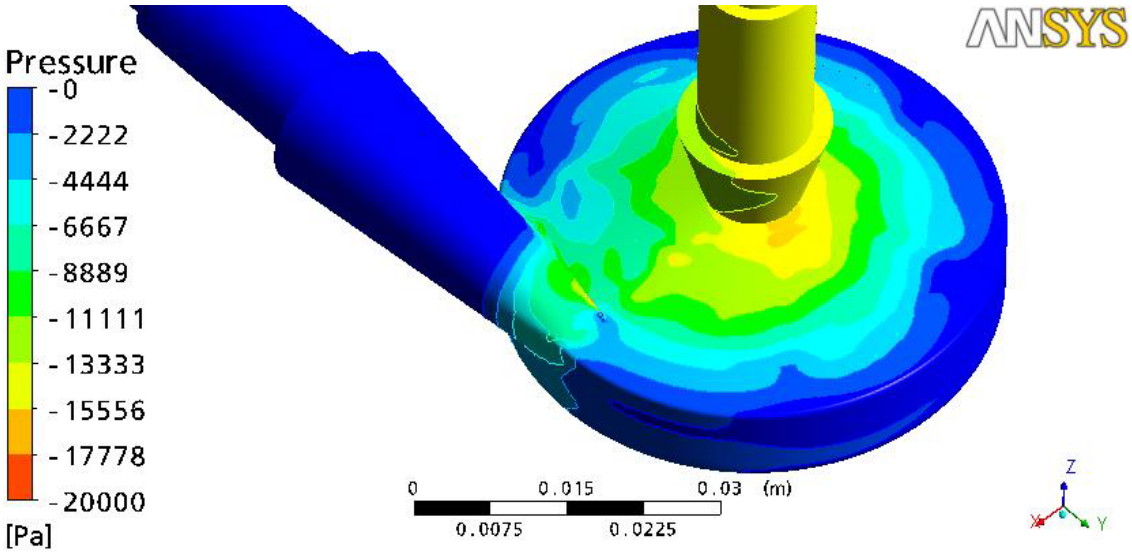

Figure 40: Pressure distribution of Model 4 (zoomed in)

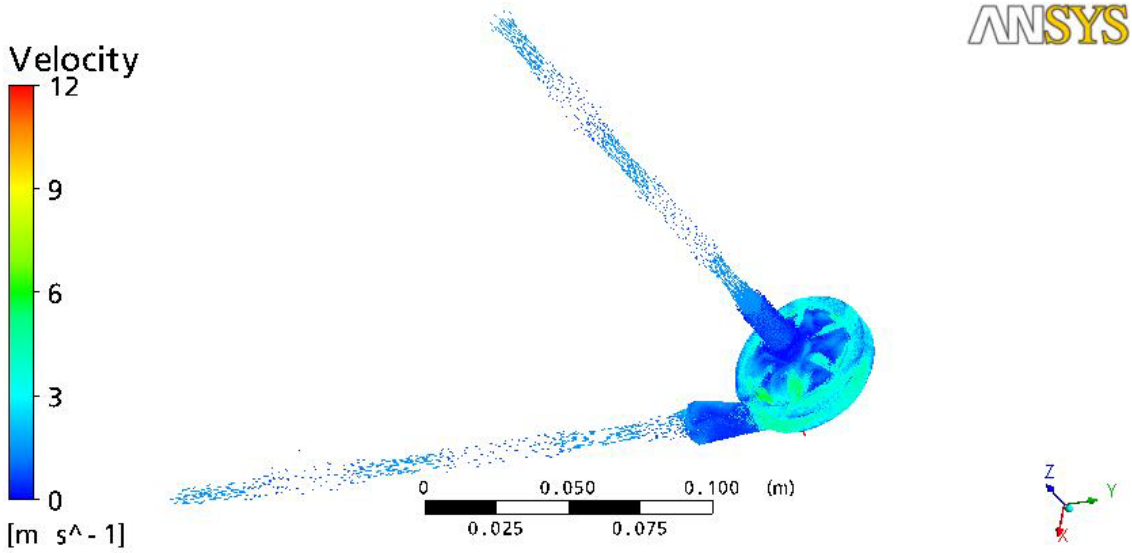

Figure 41: Velocity vectors in Model 4

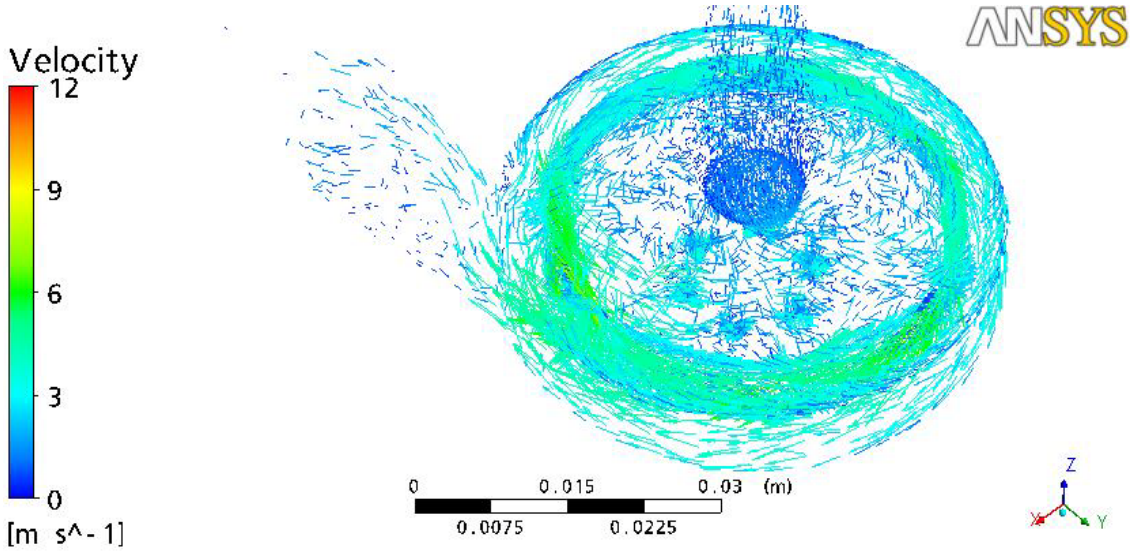

Figure 42: Velocity vectors in Model 4 (zoomed in)

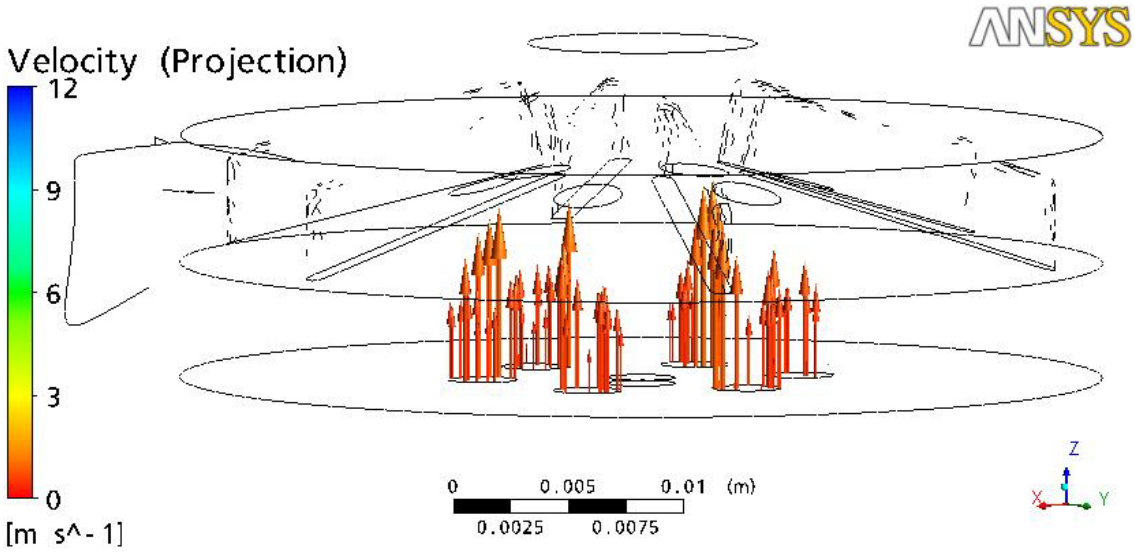

Figure 43: Velocity vectors in washout holes of Model 4

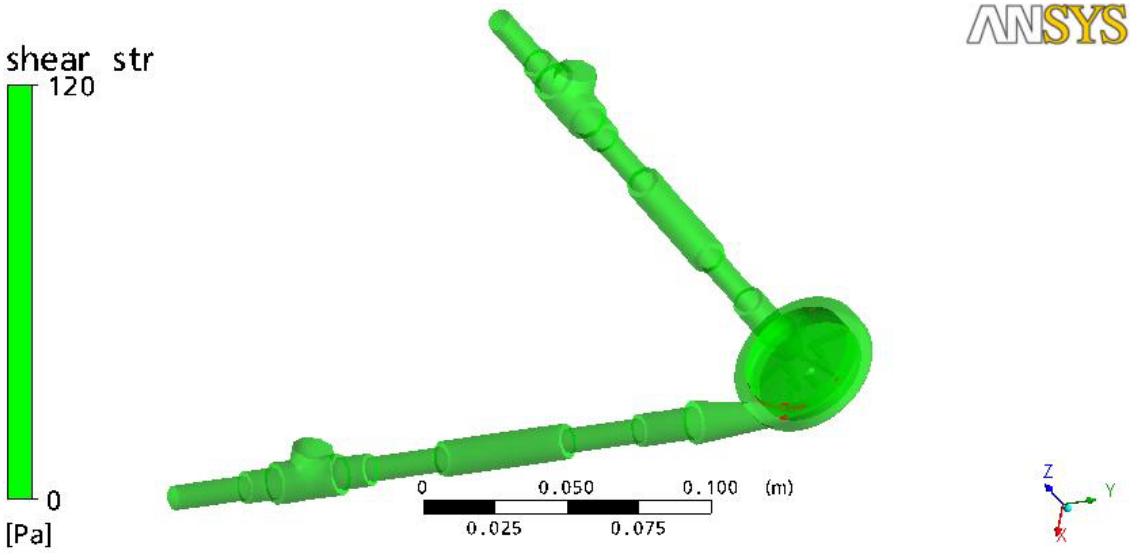

Figure 44: Shear stress distribution of Model 4

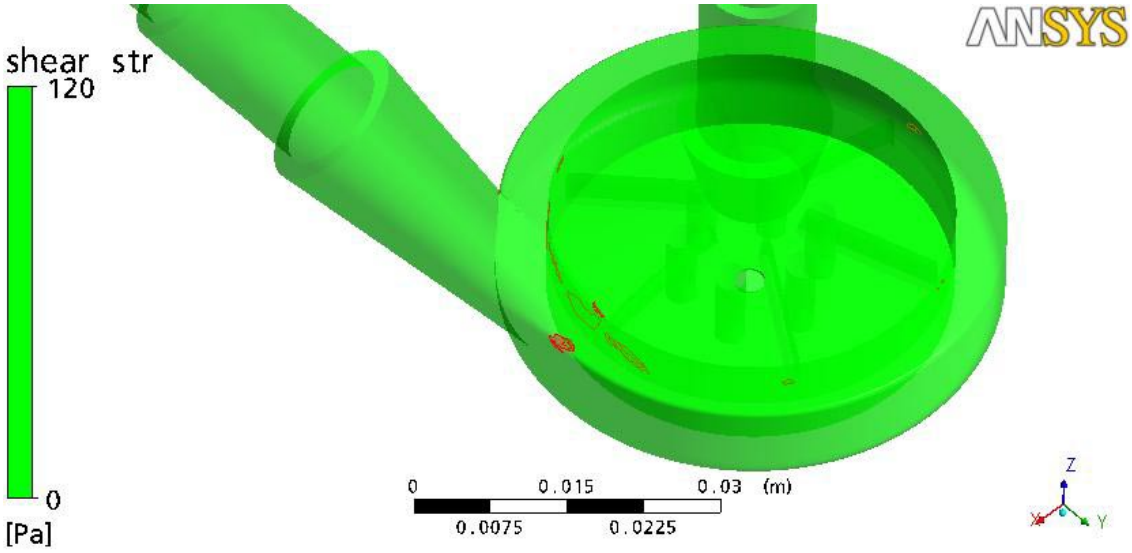

Figure 45: Shear stress distribution of Model 4 (zoomed in)

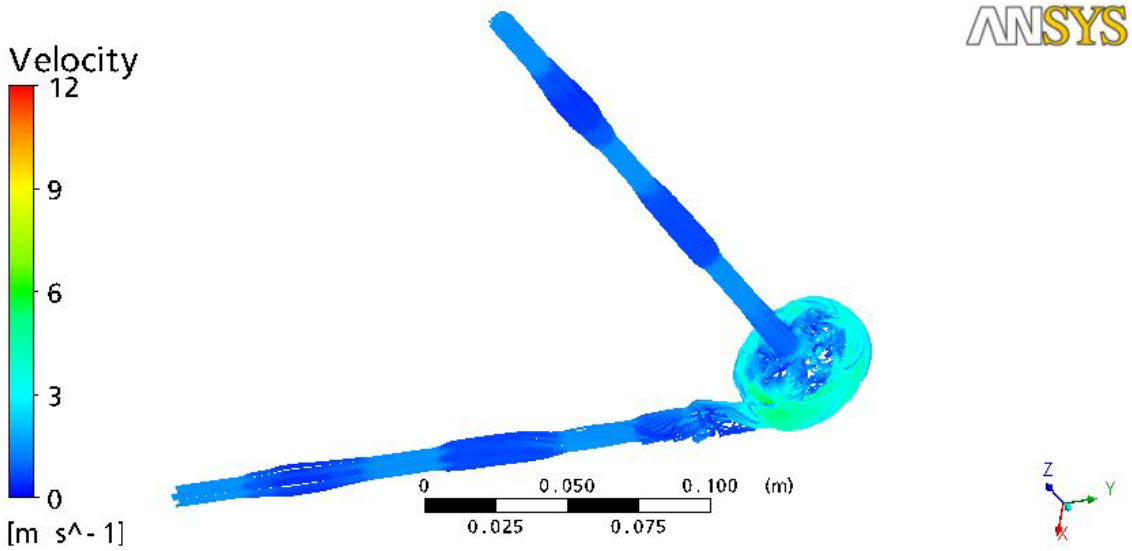

Figure 46: Streamlines in Model 4

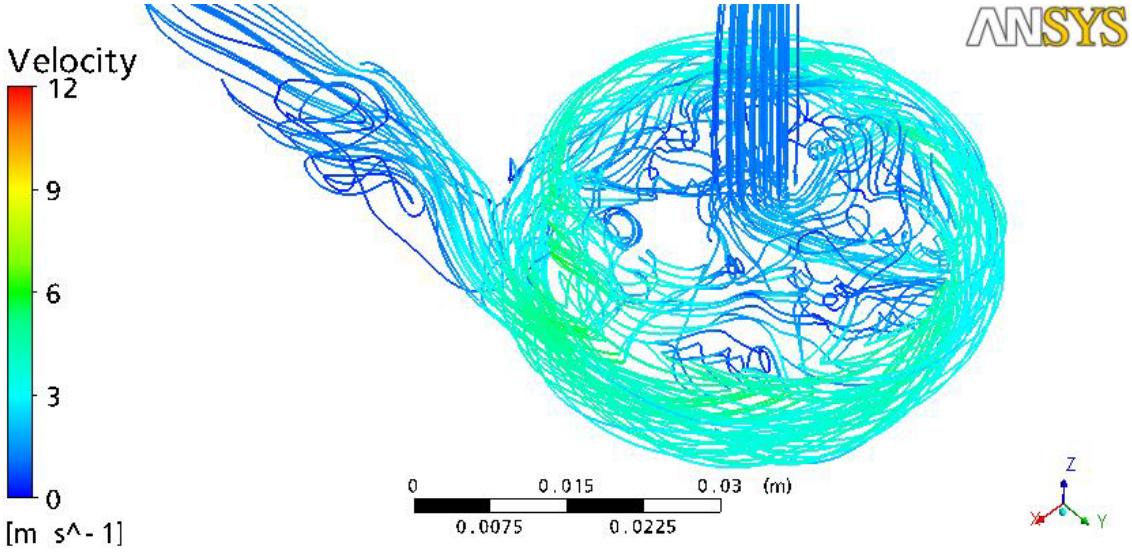

Figure 47: Streamlines in Model 4 (zoomed in)

The pressure distribution of the pump suggested that the minimum pressure occurred at the cut-water region (Figure 40), which was the geometry where fluid was separated into two parts; one of the flowing through the outlet and the other one back to the volute. The cut-water region also included high-speed flow, in accordance with the Bernoulli's principle and the high-shear stress. The velocity and shear stress values near cut-water region had important indications and will be issued below.

Velocity vectors and streamlines provided an idea about the direction and magnitude of the velocity of the flow in a any region the user interested in. In this respect, the velocity vectors in the back clearance region at the lower part of the washout holes were reviewed. The velocity vectors drawn in the projected axial direction demonstrated that the fluid was moving upwards from the back clearance region to the front side of the impeller through the washout holes (Figure 43). This way, it was proven that washout holes served the purpose of their existence by providing an active flow field in the back clearance region. Hence, the risk of

stagnation in the back clearance region was impeded. The pump was considered free of thrombogenicity since no risks were found at the most critical region of clot formation.

Shear stress distribution was investigated by introducing a critical value of 120 Pa so that the regions with shear stress over the critical value were viewed. The critical value emerged from the threshold over which hemolysis was considered risky. As seen in Figure 45, regions with shear stress values greater than 120 Pa were minor. Most of the minor risky regions were condensed near the cut-water region where high-pressure was found at. However, the streamlines with velocity variable view as in Figure 47 showed that the blood flowed within these regions with an average approximate velocity of 4-7 m/s. Assuming the dimensions of the critical regions as most 10 mm, the residence time of the fluid in the critical regions happened to be 0.0015 to 0.0025 seconds. The residence time, thus, was considered low enough to render that the blood did not traumatized in the critical region in such short residence times. This way, the pump considered carrying no risks of hemolysis.

The hydraulic efficiency (η_h) of Model 4 was calculated with respect to the procedure presented by Curtas et. al. that started with Equation 11 [16].

$$\boldsymbol{H_{th} = \frac{u_2 c_{2u}}{g}} \quad \textbf{10}$$

where u_2 and c_{2u} were calculated as in Equations 12 and 13 respectively.

$$\boldsymbol{u_2 = \omega r_2} \quad \textbf{11}$$

$$\boldsymbol{c_{2u} = u_2 - \frac{c_{2m}}{\tan(\beta_{2B})}} \quad \textbf{12}$$

$$\boldsymbol{c_{2m} = \frac{Q}{2\pi r_2 b_2}} \quad \textbf{13}$$

where c_{2m} was calculated according to Equation 14 and β_{2B} was the blade outlet angle as shown in Figure 48.

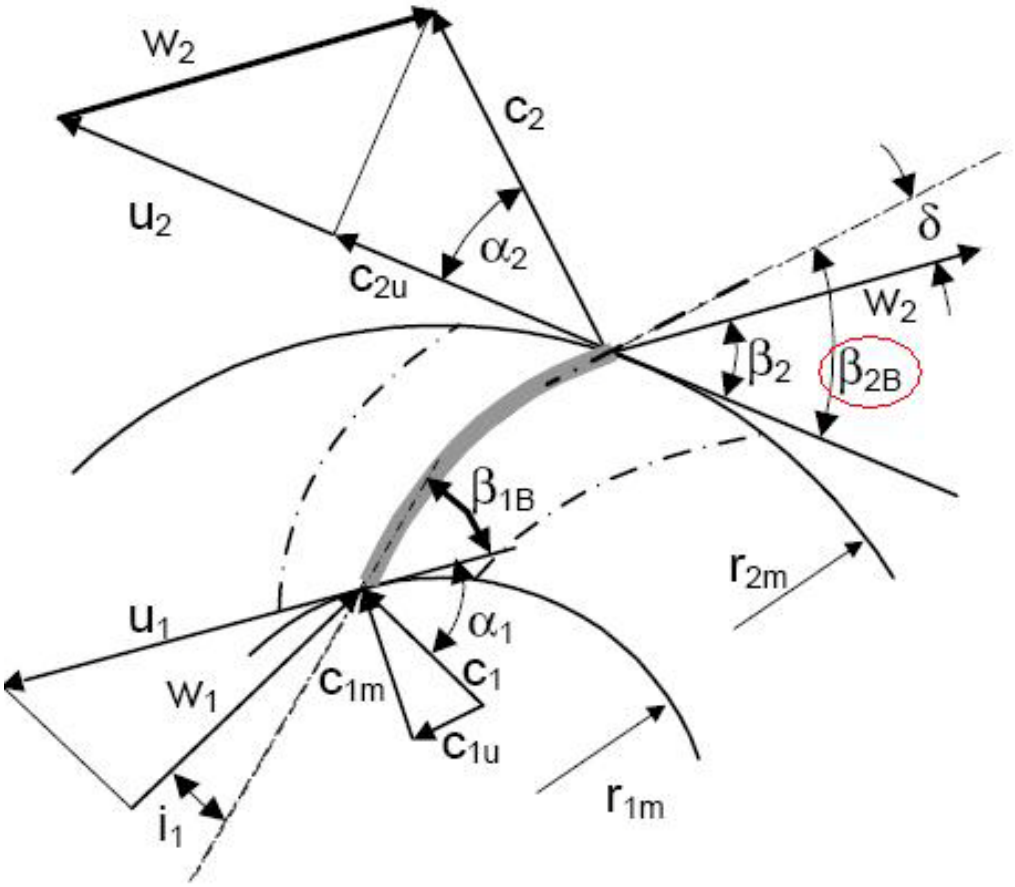

Figure 48: Blade outlet angle (β_{2B})

In calculating the efficiency of Model 4, Equation 12 was discarded since the tangent term in Equation 11 has the value of infinity due to 90 degree blade outlet angle. Hence, theoretical head of the pump was square of the circumferential speed divided by the gravitational acceleration. Theoretical head was calculated as 4.02 m while the experimental value corresponded to 1.3575 m. The hydraulic efficiency was, thus, found to be 33.8% for Model 4.

The overall efficiency was not issued up to this point of this research since there is still considerable amount of work to do in order to decrease the friction in the part between the motor and actuation of the impeller. The work included enhancing the quality of the impeller assembly, magnetic coupling and circular disk around the motor shaft. The details of this work are discussed in the future work section of the last chapter.

Chapter 5: Discussion

This chapter discusses the indications of the results and the contributions of the presented work in the general context. The subject issued in the chapter focused on the investigated design tools: one-dimensional (1-D) design procedure, Computational Fluid Dynamics (CFD) analyses and trial and error method. The reasons behind the failure or success of many results were cultivated. In addition, advantageous and disadvantageous aspects of the tools rather than the concrete results emerged from the investigation of design tools were argued.

As was presented in the results chapter, 1-D design procedure and CFD analyses were found to be incapable in assisting the design by means of determining the values of geometric design parameters of Centrifugal Blood Pumps (CBPs). On the other hand, the method of trial and error initiated with an inspiration from the findings of previous studies presented in the literature was successfully applied to the design of CBPs. This way, an enlightening document was brought into the attention of any beginner designer in the field so that the designer with no experience could handle the process easily. Therefore, the design phase in the development of a CBP was greatly accelerated. Other than that, an important amount of know-how about the design of CBPs was generated so that the future researchers on the project would be benefiting. This also will ease the future work and accelerate the progress of the project.

5.1. One-dimensional (1-D) design procedure

1-D design procedure is composed of a simplified theory that deals with mean of the mean velocities where the real flow is usually 3-D, viscous and unsteady. In order

to meet the deficit, the theory makes use of charts and empirical coefficients introduced in the equations of the procedure. The empirical coefficients and charts were emerged from vast number of experimental test data collected for a long-time. The experimental test data were mostly collected from the conventional pumps so that the valid range of the resultant coefficients and charts were of conventional pumps. That's why CBPs were out of range of the validity of 1-D design procedure. Comparatively, CBPs were considered as low specific speed, low flow rate pumps and could not take their places in the valid range of 1-D design procedure yet.

In order to cover the CBPs within the range of 1-D design procedure, there must be enough experimental test data on CBPs. However, the experimental test data present in the literature could not confront the need up to date. Although figuring the coefficients and charts out of the experimental test data (even if the data is adequate) is a difficult task, there might be tentative propositions for shortcuts in design. In this respect, the results of four pumps might provide a good reference when one attempts to use 1-D design procedure with own assumptions. The hydraulic efficiencies of four pumps were calculated with the procedure described at the end of the results chapter and yielded to a common result as in Table 7.

Table 7: Hydraulic efficiencies of presented pumps

Pump Name	**Efficiency (%)**
Model 1	36.7
Model 2	33.8
Model 3	35.2
Model 4	30.3

As the results presented in Table 7 suggests, the hydraulic efficiency might be considered somewhere between 0.30-0.37. The correlation in hydraulic efficiencies presented above should not deceive the one since the 1-D design procedure is full of

empirical coefficients and charts other than the hydraulic efficiency calculation. Moreover, the correlation in hydraulic efficiencies was achieved after experiencing test of at least four pumps where the proposed design method as a result of this thesis assumes the designer has had no experience.

In conclusion, 1-D design procedure was found to be useless in determining values of the geometric design parameters. However, the theory is still beneficial for the designer with no experience. The theory provides a qualified simple description of the behavior of the flow within the pump as well as the effects of the parameters on the flow behavior in a qualitative manner. Thereby, the theory suggests slightly good reference for an understanding of the flow behavior in the pump.

5.2. Computational Fluid Dynamics (CFD) analyses

CFD analyses were treated as a design tool since the tool simulates the real flow and presents the concluding results. This way, different designs with varying values of the geometric design parameters could be tested prior to manufacturing and the results could be utilized in design. CFD analyses employed in this research simulate the real flow by discretizing the fluid geometric into finite volume elements and solving huge matrices constituted of these elements. The governing equations to be solved were Reynolds-averaged Navier-Stokes (RANS) equations instead of a Direct Numerical Solution (DNS) of Navier-Stokes equations for most CFD applications and practice of this research. RANS represent a comparatively simplified version of the Navier-Stokes equations since DNS requires a considerable amount of computational effort beyond the facilities of our research resources. Simplification of DNS into RANS required the introduction of a turbulence model in order to close the governing equations.

The turbulence models were constituted with theoretical simplifications and empirical coefficients within the governing equations. That is why, the turbulence models were of empirical nature as was the case for 1-D design procedure. Turbulence models and the inherent coefficients were specific to the flow regime and particular geometry [30]. Although the flow regime was same for CBPs, the geometrical design of CBPs might be quite different. Since there was not any universally valid turbulence model, introduction of one turbulence model for different designs is impossible. Hence, comparison of different designs with different values of the geometric design parameters was rendered impossible in design of CBPs. So that identification of the effects of different values of the geometric design parameters was beyond the capability of employed CFD analyses. Consequently, use of CFD analyses as a design assisting tool in determining values of the geometric design parameters was out of the zone.

In order to utilize CFD analyses in determining the values of geometric design parameter prior to manufacturing, correct values must be assigned to the coefficients of turbulence models. Since the results of CFD analyses could not be checked prior to manufacturing and test of a pump, the values of turbulence model coefficients could not be assigned correctly. On the other hand, CFD analyses could be utilized in investigating the pump's inner flow after validating the tool with any other experimental result. Validation of CFD analyses in this research was accomplished by successful prediction of the pump's hydraulic performance. Later the tool was utilized for further investigation of the flow behavior within the pump. The utilization was conducted via post processing tools. In doing so, hemolytic performance and flow stagnation that causes thrombogenicity were examined. Moreover, distributions of pressure, shear stress and velocity vectors were inspected in general or in particular regions.

5.3. Trial and error method

Trial and error method is the most common design tool employed by the researchers in design of CBPs so far. In these studies, the effects of different values of the geometric design parameters in mechanical and biocompatibility performances were investigated. In general, values of the geometric design parameters to be investigated in these studies were initially set without any reasoning, possible with the insight of the researcher. The insight to guess such values with no reason requires a considerable amount of experience in design of CBPs. We, as the research group, had this kind of experience after two and a half years of research in development of Heart Turcica Centrifugal (HTC). In spite of this fact, the proposed trial and error method offer benefits for a beginner designer with no experience. As part of this method, we suggest a follow up of previous studies in the literature instead of the required experience. More specifically, the one should be assigning values of the geometrical design parameters following the knowledge gathered from previous studies as was done in this research.

One should note that in following the previous studies, the studies including designs that have same main type of pump with the designer's and presenting of successful results should be prioritized. Recommended journal articles, in this respect, specific to design of CBPs were the studies of Takano et. al. [17], Takiura et. al. [19], Masuzawa et. al. [20], Schima et. al. [29], Nishida et. al. [27] and Yoshino et. al. [50]. CFD analyses, in addition, were suggested in further investigation of the pump's inner flow proposed in a supplemental way with the proposed design method. In application of CFD analyses too, it is highly recommended to follow up previous successful studies in which the way of CFD tool employed was validated with experimental results. Recommended publications on the subject were performed by Oh et. al. [33], Zhang et. al. [34], Chua et. al. [35], Burgreen et. al. [37].

Comparing Model 4 to the pumps in the literature, 5 L/min and 100 mm-Hg pressure difference was reached at 2300 rpm rotational speed with an impeller, which has 40 mm impeller outer diameter. Many pumps in the literature indicate that reaching operating conditions of 5 L/min flow rate and 100 mm-Hg pressure difference was obtained at 2000 rpm rotational speed by impellers with 50 mm outer diameter and 3000 rpm rotational speed by impellers with 35 mm impeller outer diameter. Hence, Model 4 is not far away in performance values compared to the best ones of the literature. In addition, the smallest centrifugal blood pump that was developed for LVAD use had an impeller outer diameter of 35 mm where Model 4 has 40 mm impeller outer diameter. That is why Model 4 is considered in good dimensions since it is just 5 mm bigger in diameter than the best pump in the literature.

Model 4 also has common characteristics with most of the pumps in the literature since the common idea in the field is designing simpler pumps, i.e. radial straight blades. Model 4 has the same characteristic with a very simple design as well as the other pumps. This kind of simple design is conclusion of a considerable amount of studies, which can be found in the literature, where all indicate better hydraulic and hemolytic performances and less thrombogenicity with simpler designs. In addition to Model 4, which is considered as the best design of our group, a new pump with a distinct and peculiar design by being ultra thin is being developed by our group and results will be presented soon.

Chapter 6: Conclusions and Future Work

6.1. Concluding remarks

The design tools were examined with respect to their ability to assist the design phase of development of Centrifugal Blood Pumps (CBPs) by means of determining values of the geometric design parameters. One-dimensional (1-D) design procedure was found to be inapplicable in this respect because the range in which the tool is valid does not cover CBPs. Computational Fluid Dynamics (CFD) analyses too were inadequate to assist the design process in determining values of geometric design parameters since validation of the correctness of the tool was failed due to false prediction of the experimental results of many designs. Third, trial and error method initiated with an inspiration from the findings of previous studies was proposed. In contrast to the first two tools, proposed design method was proven to be useful after successful application of the tool to the design of two CBPs. CFD analyses, attached to the end of this design method, was utilized in investigating the pump's inner flow after its validation with experimentally measured hydraulic performance results.

In conclusion, a design methodology was generated so that the design phase in the development of CBPs could easily be handled. The proposed design methodology is most beneficial for a designer with no experience in the field. This way, future researchers of the HTC development project could easily get to better designs required for minimization and increasing efficiency of the CBPs. In addition, the accumulated experience including the presented study provides a considerable know-how to be utilized in future work of development of HTC.

6.2. Future work

The future work of the development of Heart Turcica Centrifugal (HTC) includes in-vitro test of the developed pump, Model 4, which was predicted to be successful with post-processing in CFD analyses. In-vitro test, for which the necessary equipments are being prepared, are planned to be conducted at Yeditepe University Hospital. If the in-vitro tests yields successfully results, the pump will be put in an implantable shape, i.e. a motor with smaller size will be integrated into the pump and will be sent to a clinic for in-vivo studies. If the results of in-vivo tests comes up with no problem, the pump will be ready to be an implanted to humans so that the mission of the project will be accomplished.

Other than the progress of the project with Model 4, new pumps are required to be designed in order to minimize the dimensions of the pump so that the device could be implanted in small-sized and pediatric patients. Besides, the efficiency of the pump could be enhanced so that less energy is consumed. This way, heat dissipation from the implanted device to the body could be impeded. In order to increase the efficiency, different designs with different values of the geometric design parameters could be generated. In addition, friction caused by the bearing could be minimized with more accurate manufacturing. The accuracy of manufacturing was not kept highly accurate up to date since the prior purpose was identification of the relationship with pump's geometry and hydraulic performance. Last, a study considering the magnetic coupling could be conducted to reduce the energy spent in coupling. For instance, optimum orientations of the magnets and distances between the coupled ones could be gathered by trial of different options.

Bibliography

[1] Yamane T., Ikeda T., Orita T., Tateishi T. "Fluid dynamics of turbo pumps for artificial hearts." *Material Scince and Engineering C* 4 (1996): 99-106.

[2] Nose Y. "Design and development strategy for the rotary blood pump." *Artificial Organs*, no. 22 (1998): 438-446.

[3] *World Health Organization.* 2009. http://www.who.int/cardiovascular_diseases/en/.

[4] Chua L.P., Yu S.C.M., Leo H.L., Chan W.K. "Comparison of flow characteristics of enlarged blood pump models with different impeller design." *Int. Comm. Heat Mass Transfer* 26 (1999): 369-378.

[5] *The Ministry of Health of Turkey.* 2009. http://www.saglik.gov.tr/TR/Genel/BelgeGoster.aspx?F6E10F8892433CFF404F9755767D76FF7CBB93F681A671E9.

[6] Küçükaksu S. *Türkiye' den yapay kalp pompası atağı* Anadolu Ajansı, (2006).

[7] Olsen D.B. "The history of continuous-flow blood pumps." *Artificial Organs* 24 (2000): 401-404.

[8] Yoshikawa M., Nakata K., Ohtsuka G., et al. "Feasibility of a tiny gyro centrifugal pump as an implantable ventricular assist device." *Artificial Organs* 23 (1999): 774-779.

[9] Anderson J., Wood H.G., Allaire P.E., Olsen D.B. "Numerical analysis of blood flow in the clearance regions of a continuous flow artificial heart pump." *Artificial Organs* 24 (2000): 492-500.

[10] Hoshi H., Shinshi T., Takatani S. "Third-generation blood pumps with mechanical noncontact magnetic bearings." *Artificial Organs* 30 (2006): 324-338.

[11] Nose Y., Kawahito K. "Development of a non-pulsatile permanent rotary blood pump." *European Journal of Cardio-thoracic Surgery* 11 (1997): S32-S38.

[12] Goldstein D.J., Oz M.C. *Cardiac Assist Devices.* New York: Futura, 2000.

[13] Cooley D.A. "Thirty-five years of mechanical circulatory support at teh Texas Heat Institute." *Tex Heart Inst J* 32 (2005): 168-177.

[14] Nosé Y., Yoshikawa M., Murabayashi S., Takano T. "Development of rotary blood pump technology: past, present and future." *Artificial Organs* 24 (2000): 412-420.

[15] Takatani S., Matsuda H., Hanatani A., et. al. "Mechanical circulatory support devices (MSCD) in Japan: current status and future directions." *Journal of Artificial Organs* 8 (2005): 13-27.

[16] Curtas A.R., Wood H.G., Allaire P.E., McDaniel J.C., Day S.W., Olsen D.B. "Computational fluid dynamics modeling of impeller designs for the HeartQuest left ventricular assist device." *ASAIO Journal* 48 (2002): 552-561.

[17] Takano T., Schulte-Eistrup S., Yoshikawa M., et. al. "Impeller design for a miniaturized centrifugal blood pump." *Artificial Organs* 24 (2000): 821-825.

[18] Miyazoe Y., Sawairi T., Ito K., et. al. "Computational fluid dynamic analyses to establish design process of centrifugal blood pumps." *Artificial Organs* 22 (1998): 381-385.

[19] Takiura K., Masuzawa T., Endo S., et. al. "Development of design methods of a centrifugal blood pump with in vitro tests, flow visualization and computational fluid dynamics: results in hemolysis tests." *Artificial Organs* 22 (1998): 393-398.

[20] Masuzawa T., Tsukiya T., Endo S., et. al. "Development of design methods for a centrifugal blood pump with a fluid dynamic approach: results in hemolysis tests." *Artificial Organs* 23 (1999): 757-761.

[21] Miyazoe Y., Sawairi T., Ito K., et. al. "Computational fluid dynamics analysis to establish the design process of a centrifugal blood pump: second report." *Artificial Organs* 23 (1999): 762-768.

[22] Yu S.C.M., Ng B.T.H., Chan W.K., Chua L.P. "The flow patterns within the impeller passages of a centrifugal blood pump model." *Medical Engineering & Physics* 22 (2000): 381-393.

[23] Chan W.K., Wong Y.W., Hu W. "Design considerations of volute geometry of a centrifugal blood pump." *Artificial Organs* 29 (2005): 937-948.

[24] Allaire P.E., Wood H.G., Awad R.S., Olsen D.B. "Blood flow in a continuous flow ventricular assist device." *Artificial Organs* 23 (1999): 769-773.

[25] Anderson J.B., Wood H.G., Allaire P.E., Bearnson G., Khanwilkar P. "Computational flow study of the continuous flow ventricular assist device, prototype number 3 blood pump." *Artificial Organs* 24 (2000): 377-385.

[26] Sakuma I., Sasaki T., Shiono M., et. al. "Development of a novel direct motor driven seal-less centrifugal blood pump (baylor gyro pump)." *Annu Int Conf IEEE Eng Med Biol Soc* 13 (1991): 2127-2128.

[27] Nishida M., Asztalos B., Yamane T., et. al. "Flow visualization study to improve hemocompatibility of a centrifugal blood pump." *Artificial Organs* 23 (1999): 697-703.

[28] Tsukamoto Y., Ito K., Sawairi T. "Computational fluid dynamics analysis of a centrifugal blood pump with washout holes." *Artificial Organs* 24 (2000): 648-652.

[29] Schima H., Müller M.R., Papantonis D., et. al. "Minimization of hemolysis in centrifugal blood pumps: influence of different geometries." *The International Journal of Artificial Organs* 16 (1993): 521-529.

[30] Gülich J.F. *Centrifugal pumps.* New York: Springer-Verlag, 2008.

[31] Tuzson J. *Centrifugal pump design.* New York: Wiley Interscience, 2000.

[32] Lobanoff V.S., Ross R.R. *Centrifugal pumps: design & application.* 2. Houston: Gulf Publishing Company, 1992.

[33] Oh H.W., Yoon E.S., Park M.R., Sun K., Hwang C.M. "Hydrodynamic design

and performance analysis of a centrifugal blood pump for cardiopulmonary circulation." *Proc. IMechE Part A: J. Power and Energy* 219 (2005): 525-532.

[34] Zhang J., Gellman B., Koert A., et. al. "Computational and experimental evaluation of the fluid dynamics and hemocompatibility of the CentriMag blood pump." *Artificial Organs* 30 (2006): 168-177.

[35] Chua L.P., Song G., Lim T.M., Zhou T. "Numerical analysis of the inner flow field of a biocentrifugal blood pump." *Artificial Organs* 30 (2006): 467-477.

[36] Chua L.P., Song G., Yu S.C.M., Lim T.M. "Computational fluid dynamics of gap flow in a biocentrifugal blood pump." *Artificial Organs* 29 (2005): 620-628.

[37] Burgreen G.W., Loore II H.M., Bourque K., et. al. "Computational fluid dynamics analysis of a Maglev centrifugal left ventricular assist device." *Artificial Organs* 28 (2004): 874-880.

[38] Linneweber J., Chow T.W., Takano T., et. al. "Direct detection of red blood cell fragments: a new flow cytometric method to evaluate hemolysis in blood pumps." *ASAIO Journal* 47 (2001): 533-536.

[39] Takami Y., Ohara Y., Otsuka G., Nakazawa T., Nosé Y. "Preclinical evaluation of the Kyocera Gyro centrifugal blood pump for cardiopulmonary bypass." *Perfusion* 12 (1997): 335-341.

[40] Linneweber J., Dohmen P.M., Kerzscher U., Affeld K., Nosé Y., Konertz W. "The effect of surface roughness on activation of the coagulation system and platelet adhesion in rotary blood pumps." *Artificial Organs* 31 (2007): 345-351.

[41] Coselli J.S., LeMaire S.A., Ledesma D.F., Ohtsubo S., Tayama E., Nosé Y. "Initial experience with the Nikkiso centrifugal pump during thoracoabdominal aortic aneurysm repair." *Journal of Vascular Surgery* 27 (1998): 378-383.

[42] Day S.W., McDaniel J.C., Wood H.G., Allaire P.E., Landrot N., Curtas A. "Particle image velocimetry measurements of blood velocity in a continuous flow ventricular assist device." *ASAIO Journal* 47 (2001): 406-411.

[43] Arora D., Behr M., Pasquali M. "A tensor-based measure for estimating blood

damage." *Artificial Organs* 28 (2004): 1002-1015.

[44] ASTM F1830-97: Standard practice for selection of blood for in vitro evaluation of blood pumps.

[45] ASTM F1841-97: Standard practice for assessment of hemolysis in continuous flow blood pumps.

[46] Cheremisinoff N.P. *Fluid flow, Pumps, Pipes and Channels.* Ann Arbor: Ann Arbor Science, 1981.

[47] *ANSYS Workbench.* ANSYS Inc., 2007.

[48] Fergizer J.H., Peric M. *Computational methods for fluid dynamics.* Second edition. New York: Springer-Verlag, 1999.

[49] Demir O. "Development of an implantable left ventricular assist device: Heart Turcica Centrifugal." Koc University, Istanbul, 2008.

[50] Yoshino M., Uemura M., Takahashi K., et. al. "Design and evaluation of a single-pivot supported centrifugal blood pump." *Artificial Organs* 25 (2001): 683-687.

Vita

Emre Bıyıklı was born in Konya, Turkey in 1984. He graduated from Meram Anatolian High School (old Maarif College), Konya, Turkey in 2002. He received his B.Sc. degree in Mechanical Engineering from Koc University, Istanbul, Turkey in 2007. Since then, he has enrolled in Koc University Mechanical Engineering M. Sc. program. He has been studying on the design of centrifugal blood pumps and development of a left ventricular assist device for the last two years.